

# Recent Advances in Bio-Compatible Oxygen Singlet Generation and Its Tumor Treatment

Zheng Yang Jin, Hira Fatima, Yue Zhang, Zongping Shao,\* and Xiangjian Chen\*

Light-dependent singlet oxygen ( $^1\text{O}_2$ ) produced in photodynamic therapy (PDT), is a biologically compatible reactive oxygen species showing the potential to kill tumor cells with fewer side effects on nearby normal healthy cells. The development of a high  $^1\text{O}_2$  generating photosensitizer is a particularly demanding research areas. Based on Jablonski's diagram, the photophysical factors influencing the generation of  $^1\text{O}_2$  are intersystem crossing, triplet quantum yield and life, and the singlet-triplet energy gap. Moreover, nanocarriers are also an emerging research topic with enhanced/localized delivery of photosensitizers to improve the dosage of light and enriched production of  $^1\text{O}_2$ . In this review, the production principle of  $^1\text{O}_2$  in PDT and its killing mechanism with respect to tumor cells are reviewed. In addition, the progress of PDT has been supplemented in clinical applications in recent years and the emergent preclinical tactics for prospective solutions to these challenges are discussed to improve the effectiveness and usefulness of these procedures. Moreover, the remaining research gaps and future work is outlined. This review is anticipated to heighten the research for developing new strategies for modulating the photophysical properties and improved the delivery of photosensitizers.


## 1. Introduction

Photodynamic therapy (PDT) is a minimally non-invasive cancer treatment procedure<sup>[1]</sup> that involves the activation of the

Z. Y. Jin, Y. Zhang, X. J. Chen  
The First Affiliated Hospital of Wenzhou Medical University  
Wenzhou, Zhejiang 325015, P. R. China  
E-mail: chenxiangjian@wmu.edu.cn

H. Fatima, Z. Shao  
Western Australia School of Mines: Minerals  
Energy and Chemical Engineering (WASM-MECE)  
Curtin University  
Perth, Western Australia 6102, Australia  
E-mail: zongping.shao@curtin.edu.au

Z. Shao  
State Key Laboratory of Materials-Oriented Chemical Engineering  
College of Chemical Engineering  
Nanjing Tech University  
Nanjing, Jiangsu 211816, P. R. China

 The ORCID identification number(s) for the author(s) of this article can be found under <https://doi.org/10.1002/adtp.202100176>

© 2021 The Authors. Advanced Therapeutics published by Wiley-VCH GmbH. This is an open access article under the terms of the Creative Commons Attribution License, which permits use, distribution and reproduction in any medium, provided the original work is properly cited.

DOI: 10.1002/adtp.202100176

light active materials also called photosensitizer (PSs) leads to energy transfer to nearby water or oxygen molecules, generating cytotoxic reactive oxygen species (ROS),<sup>[2-5]</sup> which can initiate the necrosis or apoptosis to kill cancer cells.<sup>[6]</sup> Compared to traditional cancer treatment techniques such as radiation, chemotherapy, and surgery, PDT showed better functionality,<sup>[7]</sup> fewer side effects,<sup>[8,9]</sup> high selectivity,<sup>[10]</sup> safe repeatability,<sup>[11]</sup> less morbidity,<sup>[12]</sup> and efficient cosmetics outcomes.<sup>[13]</sup> Moreover, PDT-based cancer treatment is more advantageous for surgical inaccessible and large-sized tumors.<sup>[14]</sup> As early as more than 20 years ago, PDT was proposed to apply in clinical practice and has been approved by the US Food and Drug Administration (FDA).<sup>[15-18]</sup> PDT has been widely used in various applications after its development, but due to the immature technical conditions, PDT was mostly used in skin diseases in the early stage, such as, psoriasis,<sup>[19]</sup> condyloma acuminatum,<sup>[20,21]</sup>

keratosis,<sup>[22,23]</sup> and various skin cancers.<sup>[23-27]</sup> Because PDT has the advantages of small invasion and low side effects, people are not willing to use it only for the treatment of skin diseases, but also try to apply it to the treatment of cancer. However, the practical applications of PDT are limited due to the following reasons; first poor PSs accumulation inside a tumor, second, limited light penetration depth, and third, the low oxygen concentration in the hypoxic core. This leads to the fact that PDT is not suitable for most solid tumors. Luckily, with the recent development of PSs, For example, the application of nanomaterials and the deep research for the modifications of nanomaterials, the limitations of clinical application of PDT have been greatly improved.

The general working principle of PDT involves the excitation of PSs with a non-toxic light<sup>[28]</sup> of an appropriate wavelength<sup>[29]</sup> which is followed by photochemical intersystem crossing (ISC) reactions of excited PSs to produce ROS. The principle of PDT and the cell death mechanism is illustrated in **Figure 1a**. The PSs in the ground state consist of two electrons with opposite spin within the lowest energy orbital. With the irradiations of light, PSs absorb light and one of these electrons jumps into a higher energy orbital without changing its spin which is named as SES of PSs. The SES PSs cannot contribute to reaction with cellular substances due to their very short lifetime (ranging from nano second to pico second). The SES PSs return to the ground state by fluorescence/heat energy or spontaneously undergo ISC where the spin of the excited electrons inverts to generate a

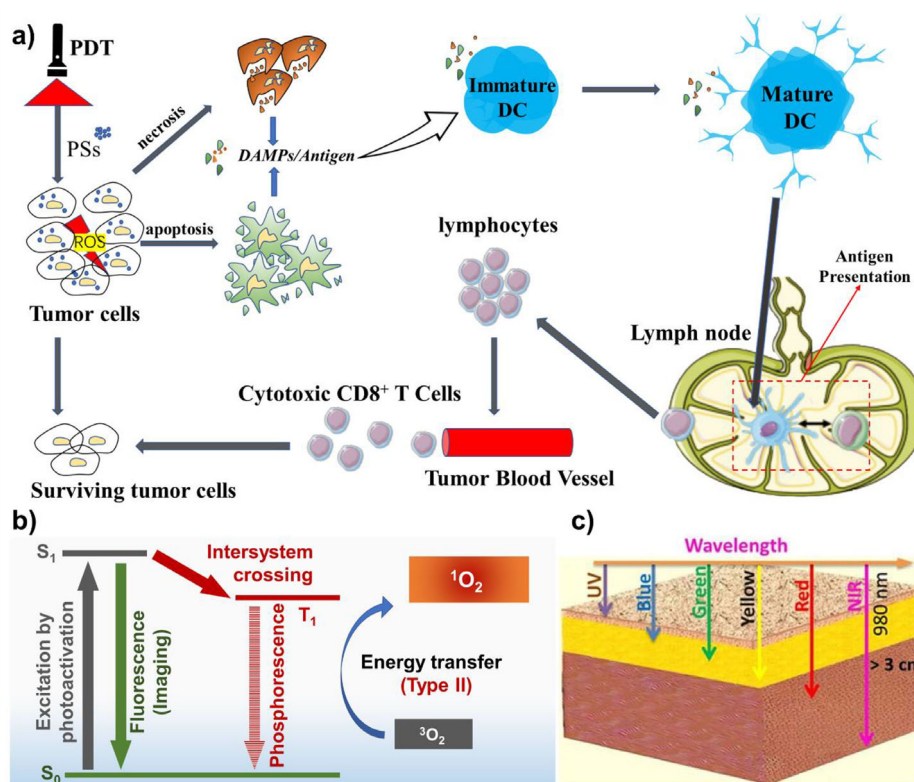


**Figure 1.** a) Mechanism of PDT in the treatment of tumors: Under specific wavelength irradiation, PS in tumor cells is activated to produce ROS, resulting in cancer cell necrosis and apoptosis. It can not only cause a strong inflammatory reaction at necrotic cells, mediate the invasion and infiltration of leukocytes to tumors, but also activate specific immunity in vivo. Specifically, tumor cells damaged by reactive oxygen species release a variety of cytokines and promote the maturation of antigen-presenting cells (mainly dendritic cells). Mature dendritic cells (DCs) spontaneously migrate to lymph nodes and provide antigens to immature T lymphocytes to promote their differentiation and maturation. The differentiated effector T lymphocytes can specifically migrate to the surviving tumor cells and kill the cells. When the immune system is activated, PDT can induce tumor immunogenic cell death (ICD). This cell death pattern is characterized by the release of immune-stimulating molecules, which can make the immune system produce long-term immune memory. It is one of the most promising methods to achieve the complete elimination of tumor cells. b) Schematic illustration of the photophysical process of PDT (Type II), and c) typical penetration depths of light as a function of wavelength. c) Reproduced with permission.<sup>[54]</sup> Copyright 2018, the authors.

corresponding triplet state population (TSP). The TSP produces ROS via Type I and Type II reactions.<sup>[30–32]</sup> Type I involves the transfer of electrons/holes in the presence of oxygen ( $O_2$ ) to generate radicals or radical ions forming less cytotoxic ROS such as superoxide anion ( $O_2^{\cdot-}$ ) which successively produces more cytotoxic ROS such as hydroxyl radicals ( $OH^{\cdot}$ ). In type II mechanism excited state PSs directly react with  $O_2$  molecules forming highly reactive ROS  $^1O_2$  via energy transfer.<sup>[33–35]</sup>

In most cases, the Type II reaction involving the generation of  $^1O_2$  preponderates<sup>[36–38]</sup> because of high reactivity,<sup>[39,40]</sup> and the moderate energy gap ( $94.3 \text{ kJ mol}^{-1}$ ) between molecular oxygen with its singlet excited state suggesting the thermal means of  $^1O_2$  production is feasible.<sup>[41]</sup>  $^1O_2$  is considered most desirable in PDT due to its oxidative ability.<sup>[42]</sup> For the first time, Min et al.<sup>[43]</sup> defined this excited state oxygen as  $^1O_2$ , consisting of higher energy, but its significance was not acknowledged until 1964 when scientists recognized its role in chemical oxidation. Furthermore,  $^1O_2$  is found to be free from other contaminants.<sup>[44]</sup>  $^1O_2$  is one of the major species responsible for the cytotoxic effects of PDT in cancerous tissues.<sup>[45]</sup> Due to its high reactivity, it causes the oxidation of the cellular macromolecules including the plasma

membrane, mitochondria, endoplasmic reticulum, nucleus, lysosomes, etc., and cell ablation happens.<sup>[46]</sup> Moreover, the  $^1O_2$  can also react with biomolecules by reversible oxidative modifications and show an important part in cellular signaling pathways, such as growth, metabolism, differentiation, and death signaling.<sup>[32,33]</sup> In conclusion,  $^1O_2$  can not only cause direct cell necrosis, but also induce programmed cell death in varying degrees, and even trigger a strong immune response (Figure 1a).

The success of PDT is highly influenced by an efficient generation of  $^1O_2$ .<sup>[47,48]</sup> Thus, a large quantity of  $^1O_2$  is needed for the enhanced therapeutic efficiency of PSs in PDT. As shown in Jablonski's diagram (Figure 1b),<sup>[49]</sup> the Type II mechanism involves the energy transfer between SES PSs and TSP to generate  $^1O_2$  that governs the phototoxicity. Therefore, high therapeutic efficiency is directly correlated with the ISC rates as the ISC is the key procedure initiating oxidative damage.<sup>[50]</sup> Usually, the ISC happens at different energy levels and the ISC generation is mainly influenced by the spin-orbital coupling (SOC) with introducing a heavy atom into the PSs.<sup>[51]</sup> Second, generating a high number of exciting triplets with a long lifetime is also beneficial in achieving enhanced  $^1O_2$  generation.<sup>[52]</sup> As the short-lived triplet shortened

the reaction duration of oxygen and PDT reagents, thus being unfavorable for  $^1\text{O}_2$  generation.<sup>[53]</sup>

It is well reported that developing a donor-acceptor system for enhanced absorption and sufficient electron transfer between donor and acceptor molecules is advantageous for enhanced ISC and the generation of long-lived triplets.<sup>[55]</sup> Third, it is also important to note the reduced energy gap between singlet and triplet PSs enables most of the singlet exciton to convert into triplet thus facilitating high ISC and improved  $^1\text{O}_2$  generation.<sup>[56]</sup> Since the  $^1\text{O}_2$  is highly reactive ROS but its short lifetime of 40 ns allows the maximum radius of reaction of 20 nm.

It is also important to emphasize that due to the short lifetime of  $^1\text{O}_2$ , they are limited in their reactivity to nearby biological media.<sup>[54]</sup> Figure 1c shows the wavelength-dependent light penetration within the biological tissues.<sup>[54]</sup> Therefore, local illumination of PSs to target tissues is an important factor as it enhances localized sensitization.<sup>[57]</sup> Moreover, it also affects the site of action of  $^1\text{O}_2$  at the subcellular level.<sup>[58]</sup> Various nanocarriers<sup>[59–61]</sup> and fiber-optic technology<sup>[62]</sup> have been developed to enhance the localization of PSs which facilitate enhanced light dosage delivery and shortened photocytotoxicity in non-targeted regions.

The efficient formation of  $^1\text{O}_2$  in the target site makes PDT a cancer strategy that can be used alone. Meanwhile, because of its unique anti-tumor mechanism, PDT can be perfectly combined with the classic treatment of cancer (chemotherapy, radiotherapy, immunotherapy, etc.). The combination therapy strategy can not only reduce the drug resistance of tumors but also reduce the side effects of treatment on the premise of ensuring the same effect. So far, PDT can be used in the treatment of most tumors. With the deepening of the study of PDT, many factors such as hypoxia which limits the efficacy of PDT have been further solved. Besides, because of its excellent antibacterial effect, PDT may become a new strategy against the recently serious drug-resistant bacteria.

There are existing reviews on  $^1\text{O}_2$  generation and their application of tumor treatment presenting the significance of  $^1\text{O}_2$ , which are incomprehensively summarized. The information's are typically gathered in the form of: i) Brief summarizing of surface functionalities and modification of PSs for enhanced  $^1\text{O}_2$  generation;<sup>[63–65]</sup> ii) or brief summarizing the detection and reactivity of  $^1\text{O}_2$  with biological molecules;<sup>[66]</sup> iii) or only focusing on the enhancement in the  $^1\text{O}_2$  generation for MOFs-based materials;<sup>[67]</sup> iv) or focusing on detection/measurement of ROS generation.<sup>[68–72]</sup>

Therefore, a critical review on the reaction of  $^1\text{O}_2$  with biological molecules, factors affecting the  $^1\text{O}_2$  generation during PDT, and their applications is still a great need. The review is organized as follows. After the introduction section which is describing the background, mechanism of PDT, and the importance of  $^1\text{O}_2$  among many other ROS molecules, the review will discuss the reaction of  $^1\text{O}_2$  with biological molecules including cytotoxic effect, cell signaling, and immune response generation in three subsections, respectively. The review then describing the photophysical factors affecting the generation of  $^1\text{O}_2$ , challenges, and strategies to improve them. We also briefly explain the immune response of PDT and combinations of various therapeutic modalities with nonoverlapping toxicities are among the commonly used strategies to improve the therapeutic index of treatments in modern oncology. The subsequent chapter will describe

the latest progress of PDT in clinical application, including the progress of oxygen-carrying PS carriers and the development of gene-encoded PSs. Finally, we introduced the antibacterial effect of PDT and clarified its great potential in solving multi-drug resistant bacteria. A summary and perspectives will also be provided at the end of this review.

## 2. The Reaction of $^1\text{O}_2$ with Biological Molecules

Within the biological media, produced  $^1\text{O}_2$  as a variety of biological functions in vivo, including cytotoxic effect produced by oxidation but also the effect of signal transduction between cells which causes a series of cellular stress responses. A low dose of  $^1\text{O}_2$  can promote cell proliferation and survival, while excessive  $^1\text{O}_2$  can directly or indirectly lead to cell death through oxidative damage to intracellular biomacromolecules (such as, protein, lipid, RNA, and DNA). Consequently, in the human organism,  $^1\text{O}_2$  is both a signal and a weapon with therapeutic potency against very different pathogens, such as microbes, viruses, cancer cells, and thrombi. It can not only produce a direct cytotoxic effect but also induce programmed cell death through a variety of signaling pathways, causing a strong immune response.

### 2.1. Cytotoxic Effect Produced by $^1\text{O}_2$

Owing to high reactivity,  $^1\text{O}_2$  can react with several organelles, and resulting in modifications within key cellular targets, including unsaturated lipids, guanine for nucleic acids, and targeted amino acids.<sup>[73]</sup>

#### 2.1.1. Cytotoxic Effect of $^1\text{O}_2$ on the Cell Membrane

The cell membrane consists of three main components including phospholipid, glycoprotein, glycolipid, and protein. Among them, phospholipids are the basic scaffold of the cell membrane and are also important targets for  $^1\text{O}_2$ .<sup>[74]</sup> These oxidative reactions have antimicrobial effects that are fundamental to PDT in cancer treatment.<sup>[75]</sup> Generally, the sn-2 position of phospholipids is esterified to unsaturated fatty acids, and subsequently, the unsaturated fatty acids can be further oxidized by  $^1\text{O}_2$  to form phospholipid hydroperoxides (PL-OOH).  $^1\text{O}_2$  can produce concentrated hydrogen peroxide isomers by an addition reaction. During this reaction, several important intermediates of non-radical peroxidation are produced, including lipid hydroperoxides (LOOHs) and cholesterol hydroperoxides (ChOOHs).<sup>[74]</sup> The generated LOOHs can participate in cell signal transduction and trigger a series of reactions through a variety of energy conversion/electron migration pathways.<sup>[76]</sup> Figure 2a showed the possible routes of LOOH formation and turnover in photodynamic activated cells.<sup>[74]</sup>

Some LOOHs are effectively reduced to corresponding alcohols by several peroxidases (Prx), such as, glutathione peroxidase peroxidases (GPx). Other LOOHs, which cannot be effectively reduced by Prx enzyme, can be oxidized with free metal ions, heme protein, and other biological oxidants to produce highly active free radical intermediates including peroxides ( $\text{loo}\cdot$ ) and alkoxyls

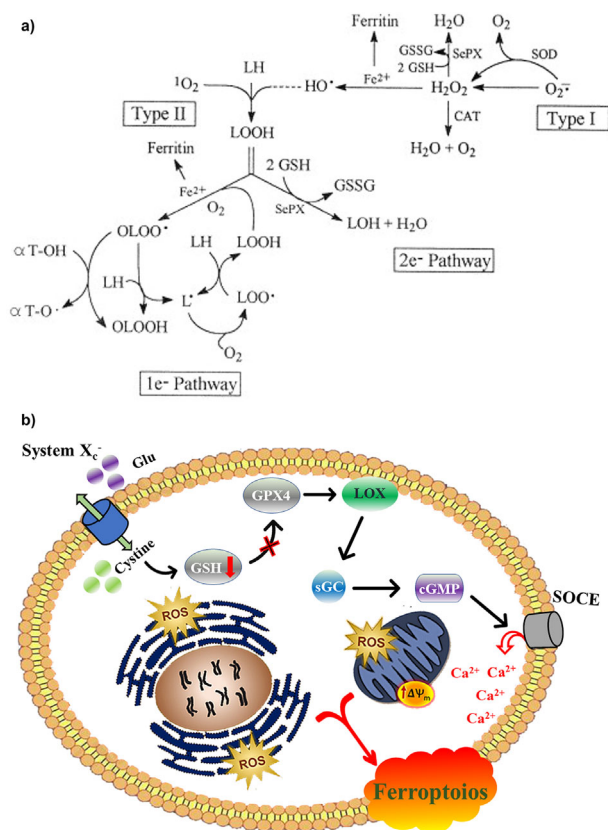


**Figure 2.** a) Diagram showing possible routes of LOOH formation and turnover in photodynamic activated cells. b) Mechanism of iron-dependent, oxidative death. a) Reproduced with permission.<sup>[74]</sup> Copyright 2001, Elsevier Science B.V.

(LO $\cdot$ ).<sup>[77,78]</sup> These free radicals can cause irreversible damage to a variety of important components (proteins, nucleic acids, etc.) in cells, thus changing the normal cell function. In addition,  $^1O_2$  mediated iron-dependent ROS generation and lipid oxidation can lead to a novel type of cell death named ferroptosis.<sup>[79]</sup> Furthermore, the inhibition of the cystine/glutamate antiporter (system x(c) (-)), will create a void in the antioxidant defenses of the cell and ultimately leading to iron-dependent, oxidative death (Figure 2b). Ferroptosis is closely related to oxidative reaction, and it is an important part of cell apoptosis. System X<sub>c</sub><sup>-</sup> absorbs cystine and reverses the transport of glutathione (Glu), resulting in the decrease of intracellular Glu concentration. Next, GSH-dependent enzyme GSH peroxidase 4 (GPX4) was also inhibited. Inhibition of GPx4 leads to the activation of lipoxygenase (LOX), which produces a large amount of ROS in mitochondria and the endoplasmic reticulum. In addition, the hyperpolarization of mitochondrial membrane potential ( $\Delta\Psi_m$ ) can lead to an exponential increase in ROS production. LOX metabolites can induce the activation of soluble guanylate cyclase to form cGMP accumulation, and then activate calcium channels, leading to calcium influx. These processes can further accelerate apoptosis.

In addition to phospholipids, cholesterol is also one of the main components of biofilms, which plays an important role in regulating the physical properties of the membrane and regulating a variety of signaling pathways.<sup>[80]</sup> Cholesterol can be

peroxidized by  $^1O_2$ , in which cholesterol-5 $\alpha$ -hydrogen (5 $\alpha$ -OOH) peroxide is one of the main products of photosensitive peroxidation. Although many antioxidant mechanisms in the human body can antagonize the cytotoxic effect of cholesterol oxidation, 5 $\alpha$ -OOH is still one of the most noxious of the natural lipid hydroperoxides known at present. Furthermore, ChOOHs are capable of spontaneous translocation. The speed of transferring from donor membrane/lipoprotein to receptor membrane/lipoprotein is much faster than PLOOHs with the same peroxide content.<sup>[81]</sup> In this case, as a cytotoxic oxidant, the scope of cytotoxicity of ChOOHs has been greatly improved. The experiments showed that after cholesterol is oxidized by  $^1O_2$ , the stimulated cells will transport more peroxides to mitochondria, which will aggravate the loss of membrane potential and then cause more extensive apoptosis.<sup>[82]</sup>

### 2.1.2. Cytotoxic Effect of $^1O_2$ on the Nucleus

The nucleus is the most important organelle of a cell, which contains the genetic material called nucleic acid. If the nucleus is destroyed by oxidation, it will cause devastating damage to the cell itself, which will cause irreversible cell death and ROS can react with a variety of nucleobases and sugar groups in nucleic acids to destroy the original structure of the nucleus.<sup>[83–86]</sup>  $^1O_2$  is found to be an extremely destructive oxidants for cellular DNA due to its high reactivity.<sup>[87,88]</sup> The survival time of  $^1O_2$  in the cell environment is a key parameter to determine the efficiency of DNA oxidative damage in the nucleus. This value is estimated in a few  $\mu s$ , and it will be extended or shortened with the change of  $^1O_2$  generation position. After generation,  $^1O_2$  will be consumed by physical quenching and chemical reactions (including oxidation with unsaturated lipids and other intracellular substances).<sup>[89,90]</sup>

$^1O_2$  can react with many components in the nucleus to induce apoptosis/death, mainly the base pairs in DNA. Unlike other oxidants-mediated reactions (including  $\bullet OH$  and one-electron oxidants), guanine is the preferential target among the pyrimidine and purine bases of  $^1O_2$ -mediated oxidation reactions.<sup>[83]</sup> In the experiment of purine and pyrimidine nucleotides exposed to UVA-excited methylene blue (MB), the guanine base pairs in deoxyguanosine acid reacted preferentially with  $^1O_2$ , while the other three types of deoxynucleotides (dAMP, dTMP, dCMP) were not found to be affected.<sup>[91]</sup> Recent theoretical studies have further proved that guanine can react with  $^1O_2$  as a classical base pair of DNAs.<sup>[92,93]</sup>

### 2.1.3. Cytotoxic Effect of $^1O_2$ on the Mitochondrion

Mitochondria are important organelles in most cells and are the main places for aerobic respiration. Therefore, when mitochondria are damaged, cells will lose the energy source for normal life activities and eventually die. Mitochondria not only provide energy for cells but also regulate cell growth and cell cycle by participating in cell differentiation, cell information transmission, and cell apoptosis. When cells are under oxidative stress, some evidence suggests that the mitochondrial-ROS-driven feed-forward loop might increase phospho-PDGFR $\alpha/\beta$ . And then, the phosphorylation of this signaling pathway can stimulate apoptosis

by inhibiting PI3K-Akt pathway.<sup>[94]</sup> Furthermore, the damage of mitochondria will affect the energy metabolism of cells. The increase of mitochondrial membrane permeability can also release apoptosis-inducing factors and other molecules into the cytoplasmic matrix, destroy cell structure, and control programmed cell death. One of the most important reasons for these pathological changes is the oxidation reaction mediated by  $^1\text{O}_2$ . In addition,  $^1\text{O}_2$  is also involved in the mutation of mt DNA, resulting in mitochondrial dysfunction.<sup>[95]</sup> With the deepening of research, the role of mitochondria in apoptosis has attracted more and more attention. Consequently, mitochondria have become a popular sub-cellular organelle for PDT targeting.

## 2.2. Cellular Signaling Regulated by $^1\text{O}_2$

$^1\text{O}_2$  not only directly damage biological macromolecules such as cell membrane, nucleus, and mitochondria,<sup>[96,97]</sup> but also activate apoptotic signal pathway to induce cancer cell death (Figure 3a).<sup>[98]</sup> In response to oxidative stress, some tumor cells can antagonize  $^1\text{O}_2$ -induced apoptosis by increasing the expression of antioxidant enzymes. Accordingly, the amount, location, and duration of  $^1\text{O}_2$  production also activate different signaling pathways in cells. This will determine the response of tumor cells to  $^1\text{O}_2$  and the overall therapeutic effect.

### 2.2.1. Oncogenic Signaling Regulation of $^1\text{O}_2$

Akt (also known as protein kinase B) is a proto-oncogene activated in a variety of cancers and has anti-apoptotic effects in response to a variety of stimuli such as radiotherapy, hypoxia, and chemotherapy.<sup>[99]</sup> It has been proved that the activation of PI3K/Akt and its downstream signaling pathway directly affects cell proliferation/apoptosis. It makes this signaling pathway play an important role in the regulation of tumorigenesis. On the one hand, it promotes the secretion of matrix metalloproteinase-9<sup>[100]</sup> and induces epithelial-mesenchymal transition<sup>[101]</sup> to enhance the invasiveness of cancer cells and induce their metastasis. On the other hand, it can enhance telomerase activity and replication by activating telomerase reverse transcriptase and increase the ability of tumor self-healing.<sup>[102]</sup> The increase of  $^1\text{O}_2$  concentration can lead to the inactivation of PTEN (a tumor suppressor gene frequently deleted or mutated in many human cancers) and change the kinase-phosphatase balance. These reactions can promote the growth of tumor through Akt activated tyrosine kinase receptor-mediated signal transduction. In addition, Akt can inactivate several key cell targets (Bad, forkhead transcription factors, and c-Raf and caspase-9) through phosphorylation, which will further antagonize the apoptosis of cancer cells.<sup>[103]</sup>

### 2.2.2. Apoptotic Signaling Upon $^1\text{O}_2$

The intercellular apoptosis signal of tumor cells is mainly mediated by HOCl and NO/peroxynitrite signaling pathways.<sup>[104,105]</sup> However, malignant cells continuously produce extracellular superoxide anion under the control of activated oncogenes and highly express catalase. These changes may protect cancer cells

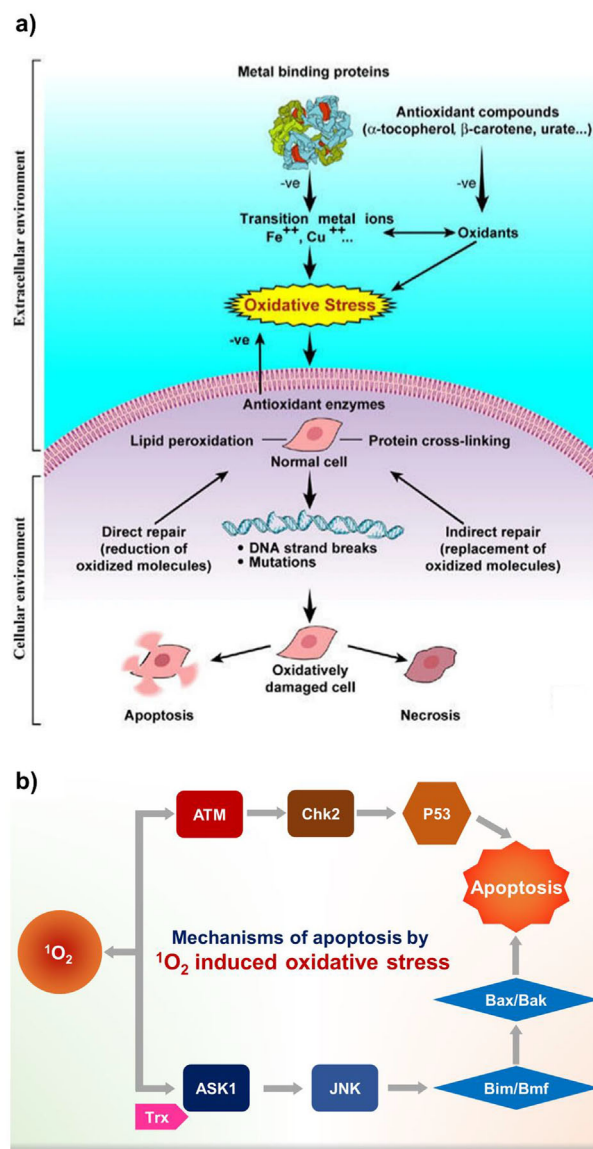


**Figure 3.** a) Mechanisms of oxidative stress-induced cell death. b) Mechanisms of apoptosis by  $^1\text{O}_2$  induced oxidative stress. a) Reproduced according to the terms of the CC-BY license.<sup>[98]</sup> Copyright 2005, The Authors.

from apoptosis mediated by HOCl and NO/peroxynitrite signaling pathways. Under the action of sufficient amounts of  $^1\text{O}_2$ , the protective catalase highly expressed by tumor cells would be inactivated, which would then reactivate the HOCl and NO/peroxynitrite signaling pathways and induce tumor cell apoptosis.<sup>[106,107]</sup> Other studies have shown that  $^1\text{O}_2$  can oxidize histidine residues in the active center, resulting in the inactivation of antioxidant enzymes.<sup>[108]</sup> Moreover,  $^1\text{O}_2$  can inactivate the highly expressed catalase on tumor surface. These catalases can protect tumor cells from ROS-mediated apoptosis. Consequently,  $^1\text{O}_2$  counteracts part of the anti-apoptotic ability of the tumor.<sup>[109]</sup>

Apoptosis signal-regulating kinase 1 (ASK1), one of the members of the mitogen-activated protein kinase kinase kinase family, plays a very important role in regulating the process of

apoptosis. Oxidative stress caused by  $^1\text{O}_2$  can stimulate ASK1 activation and exert physiological functions.<sup>[110]</sup> It would activate c-Jun N-terminal kinase (JNK) and p38MAPK pathways to induce apoptosis via mitochondria-dependent activation of caspase-9 and caspase-3.<sup>[111]</sup> Thioredoxin (Trx) can directly inhibit ASK1 activity by inducing ASK1 ubiquitination, besides, binding of the reduced form of TRX to ASK1 also exerts an inhibitory effect. When TRX is oxidized by  $^1\text{O}_2$ , the site where it binds to ASK1 will undergo structural changes, leading to the separation.<sup>[112]</sup>

Subsequently, ASK1 is activated by homo-oligomerization and auto-phosphorylation. Bim is a cell death mediator that interacts with Bcl-2 (B-cell lymphoma-2, one of the most important oncogenes in the study of apoptosis). Bmf is a modification factor of Bcl-2. Both of them can be phosphorylated by ASK1-activated JNK and further activate the downstream protein receptor (Bak/Bax) of the pathway to initiate apoptosis, respectively.<sup>[113]</sup> In addition,  $^1\text{O}_2$  can regulate apoptosis by regulating ataxia telangiectasia mutated (ATM). Then ATM induces DNA-oxidative damage and cell apoptosis by activating atm-chk2-p53 signaling pathway (Figure 3b).

### 3. Strategies for Enhanced Photosensitized $^1\text{O}_2$ Generation

This section summarizes the recent development and strategies for enhanced  $\Phi_{\Delta}$  under 3 categories depending upon the photo-physical properties of PSs molecule, that is, enhanced ISC, enhanced *triplet quantum yield and life*, and reducing the singlet-triplet energy gap.

#### 3.1. Enhanced Intersystem Crossing

A primary challenge of achieving high  $\Phi_{\Delta}$  is to maximize the singlet-triplet ISC rates as it involves the energy transfer between the excited triplet and ground-state molecular oxygen. It is well reported that the enhancement in ISC rates can be achieved with the increase in SOC by introducing a heavy atom into the PSs.<sup>[51,114]</sup> This mechanism is named a spin-orbit coupling ISC (SOC-ISC). Thus, a controlled synthesis and design of heavy atom-based PSs can significantly enhance the ISC and improve the  $\Phi_{\Delta}$ . It involves the mixing of two pure electronic states by SOC and altering the atomic energy level of electrons. The photo-physical properties of SOC-ISC are illustrated in **Figure 4a**.

Generally, the SOC-ISC is attained by the internal heavy atom effect with a direct covalent bonding of heavy atom and PSs molecule.<sup>[115]</sup> For example, the intra-cyclic sulphur of thionine by oxygen and selenium increases the SOC between the  $\pi\pi^*$  electronic states, thus producing high ISC.<sup>[116]</sup> However, the internal heavy atom effect requires complicated synthesis and undesirable modification of PSs which drop the  $\tau_T$  and large atomic radii of heavy atoms distort the structure of parent PSs thus losing the sensitizer planarity.<sup>[117]</sup> In this respect, the external heavy atom effect generated by the intermolecular external bonding appears to be an advantageous alternative, discovered by Kasha in 1952.<sup>[118]</sup> The external heavy atom weakens the spin prohibition thus increasing the absorbance values and enhancing the ISC rate.<sup>[119]</sup> Gorman et al.<sup>[18]</sup> presented a more than 1000 times increase in PDT efficacy using nitrogen-bridged two-pyrrole due

to external heavy atom effect in comparison with internal heavy atom effect.

Various metals have been studied in past as promising heavy atoms.<sup>[120,121]</sup> For example, Zhou et al.<sup>[122]</sup> developed Au(III) or Pt(IV) conjugated hypocrellin A (HA) as a natural perylene quinine PSs. To investigate the heavy atom effect their fluorescence spectra and time-resolved fluorescence measurements were recorded. The fluorescence spectra showed a reduction in fluorescence intensity of Pt/HA and Au/HA as compared with HA. Moreover, time-resolved fluorescence measurements also suggested the reducing fluorescence lifetime of Au/HA and Pt/HA comparing with HA. However, the high cost and toxicity involved with metal atoms limited their practical applications in PDT.<sup>[123]</sup> Recently, the density functional calculations and an overlapped wave function of host and guest molecules presented an enhanced SOC with the conjugation of halogen atoms, that is, a heavy atom<sup>[124–126]</sup> which follows the deactivation path of  $S_0 \rightarrow S_1 \rightarrow T_1$ .<sup>[127]</sup> This mechanism was first discovered by McClure in 1949.<sup>[128]</sup> Zou et al.<sup>[129]</sup> developed a series of BODIPY derivatives (Figure 4b) with the conjugation of pyrrole hydrogen atoms with BODIPY and halogen atoms (Br, I). A significant increase in  $\Phi_{\Delta}$  was observed with the introduction of halogen atoms. In another study, iodine substituted silica/porphyrin nanoparticles were developed with high photostability. The as-synthesized nanoparticles showed improved  $\Phi_{\Delta} = 0.52$ .<sup>[130]</sup> Quartarolo et al.<sup>[131]</sup> developed Br substituted porphyrin derived PSs with enhanced ISC efficacy and high  $\Phi_{\Delta}$ , that is,  $\Phi_{\Delta, \text{hal}} = 0.56\text{--}0.64$ ,  $\Phi_{\Delta, \text{non-hal}} = 0.49$  due to SOC.

Several factors are affecting the enhancement in the SOC rate by the conjugation of halogen atoms such as the position,<sup>[132,133]</sup> the atomic number,<sup>[133]</sup> bond length<sup>[134]</sup> of the halogen atom. Simon et al.<sup>[135]</sup> displayed a considerable enhancement in the SOC rate and  $\Phi_{\Delta}$  when halogen atoms reside in the core region. In another study, Belfield et al.<sup>[136]</sup> investigated the optimized position of the halogen atom in BODIPY core for enhanced  $\Phi_{\Delta}$ . The results confirmed that substitution at the 2, 6 positions could significantly improve the SOC that is due to the slow activation of the heavy atom effect in the core region. In general, the enhancement in ISC is typically attained by conjugating the halogen without disrupting the planarity of the PSs.<sup>[132]</sup> Furthermore, in most cases, ISC transition time decreases sharply with the increase in the atomic weight of halogen and the number of halogen atoms.<sup>[132,133]</sup> For example, the iodine atom possesses high efficiency than bromine.<sup>[132]</sup> Furthermore, the distance between the halogen atom and the PSs molecules also contributes toward the enhancement efficiency.<sup>[137]</sup> Ang et al.<sup>[134]</sup> conducted a computational study to investigate the extent to which ISC is enhanced with halogen atom bonding length with benzaldehyde. The results demonstrated a profound decrease in SOC with the increase in the bond length of the halogen atom.

In addition to the external heavy atom effect, halogen bonded PSs showed several other beneficial characteristics, that is, enhanced hydrophilicity and passive targeting of tumor.<sup>[138]</sup> Arme' nio et al.<sup>[139]</sup> investigated the cytotoxicity of WiDr colorectal adenocarcinoma and A375 melanoma cancer cells using halogenated derivative PSs. The in-vitro activity of these materials presented 5–10 times higher inhibition of tumor growth. In another study, iodine-containing silica nanoparticles were developed for

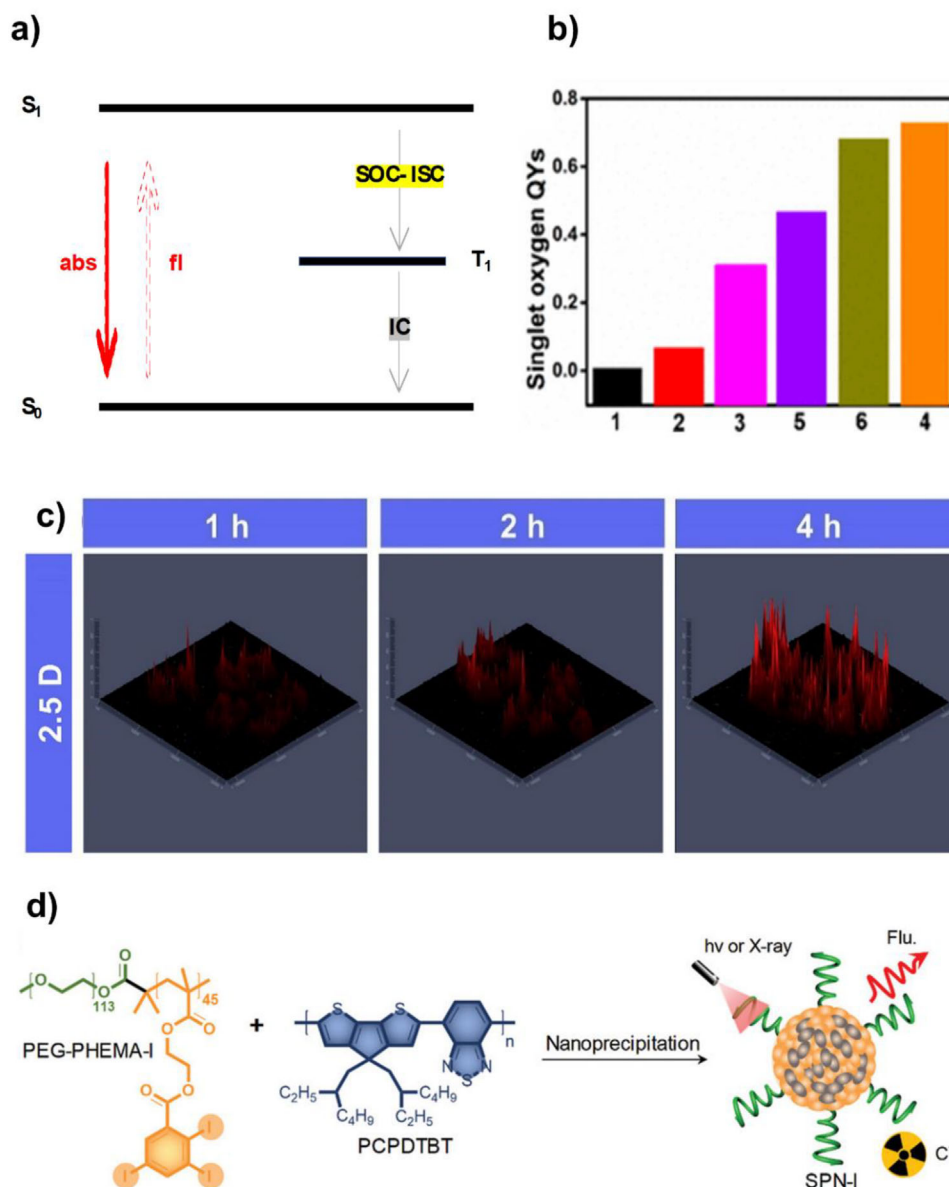


**Figure 4.** a) Jablonski diagram illustrating  $S_0$ —ground state,  $S_1$ —lowest singlet excited state,  $T_1$ —lowest triplet excited state. Solid arrow representing most likely processes and dashed arrow representing less likely process. b)  $^1\text{O}_2$  generation by six compounds (BODIPY derivatives), c) relative fluorescence intensity of HeLa cells for different periods (1, 2, and 4 h), incubated with SNBDP NPs (20.0  $\mu\text{M}$ ) under the excitation of the red channel, scale bars: 20  $\mu\text{m}$ , d) schematic illustration for the preparation of SPN-I. b) Reproduced with permission.<sup>[129]</sup> Copyright 2017, American Chemical Society. c) Reproduced with permission.<sup>[141]</sup> Copyright 2020, Elsevier Ltd. d) Reproduced with permission.<sup>[142]</sup> Copyright 2020, WILEY-VCH.

improved in vitro PDT efficacy.<sup>[140]</sup> Recently, Zhang et al.<sup>[141]</sup> studied the heavy atom effect for the efficient killing of Hella cells by PDT due to decent  $\Phi_{\Delta}$  (40%). The internalization and imaging properties of the PSs were further investigated using a laser scanning microscope at different time intervals. The bright red signal suggested profound endocytosis and internalization of halogenated PSs by HeLa cells which tend to increase in its intensity with time (Figure 4c). Zhou et al.<sup>[142]</sup> developed an iodine conjugated semiconductor polymer material (SPN-I) by nanoprecipitation method as shown in Figure 4d. The developed material showed an enhanced ISC due to the presence of a high-density heavy atom, that is, iodine. Furthermore, the tumor inhibition

rate was about 98.7%, showing high PDT efficacy and zero dark side effects.

Despite the advantageous ISC rate with heavy atom effect, they largely have a disadvantage of dark toxicity for PSs that is the major concern for the PSs synthesis and applications in PDT. Zhou et al.<sup>[143]</sup> investigated the effect of halogen heavy atom effect on the dark toxicity and cell viability of HepG2 cells. The results presented 87% cell viability in dark and a dramatic diminution of cells after light irradiation suggesting high biocompatibility and cytotoxicity. Therefore, introducing heavy atoms is not ideal to attain improve ISC, unless effective suppression of dark toxicity. The general approach to developing heavy atom-free PSs is

to attain a similar energy level of S1 and TSP or proper appropriate molecular geometry to mollify the reserved momentum in ISC.<sup>[144]</sup> Hussein et al.<sup>[145]</sup> for the first time reported the heavy atom free thionated naphthalenediimide (NDI) derivatives with enhanced ISC and high of  $\Phi_{\Delta}$  of 56% due to  $^1(\pi-\pi)^* \rightarrow ^3(n-\pi)^*$  transitioning. Nguyen et al.<sup>[146]</sup> prepared sulphur substituted NDI by one-pot synthesis to achieve enhanced SOC rate and high  $^1O_2$  generation due to enhancement in electron-donating potential of NDI.

### 3.2. Enhanced Triplet Quantum Yield and Life

The heavy atom effect is a general strategy for improving the  $\Phi_{\Delta}$ , however, it may introduce several problems such as tedious synthesis, low solubility PS, high cost, and dark toxicity.<sup>[147]</sup> Moreover, the  $\tau_T$  is also shortened as the heavy atom effect enhances both the  $S_1 \rightarrow T_1$  and the  $T_1 \rightarrow S_0$  processes. Thus, high  $\tau_T$  is desired.

Photoinduced electron transfer is an attractive advantageous strategy of enhancing ISC using electron acceptor–donor subunits, producing high  $\tau_T$ .<sup>[52,148]</sup> The main idea is the chemical or physical adsorption of donor molecules showing a high absorption coefficient with an acceptor molecule for an effective energy transfer, enhanced ISC, and improved  $\tau_T$  and  $\Phi_T$ .<sup>[55]</sup> The electronic structure of electron donor and acceptor molecules offers the possibility to absorb light, transfer the electrons from donor to acceptor molecule, and generate a highly dipolar state named as charge transfer state.<sup>[149]</sup> The magnitude of charge transfer can be assessed by the excited state dipole moment which tends to increase with the increase in charge transfer.<sup>[150,151]</sup> It has been reported that the charge transfer state undergoes ISC through two main processes, that is, radical-pair ISC (RP-ISC)<sup>[152]</sup> and spin-orbit charge transfer ISC (SOCT-ISC).<sup>[153]</sup> Figure 5a shows the schematic illustration of both RP-ISC and SOCT-ISC processes. ISC in the first formed singlet charge transfer state ( $^1CT$ ) occurs through hyperfine interaction—an interaction between an electron spin and a nuclear spin which followed by the formation of an intermediate triplet charge-transfer state ( $^3CT$ ) or fast charge recombination forming the lowest triplet excited state.<sup>[154]</sup> This mechanism is called RP-ISC. Zhijia et al.<sup>[155]</sup> developed NDI and NDI conjugated 2,2,6,6-tetramethylpiperidinyloxy (TEMPO) dyads showing the RP-ISC mechanism. A broad and structureless fluorescence spectra at around 630 nm have been observed for NDI which significantly quenched with the conjugation of TEMPO (Figure 5b), due to the occurrence of photoinduced electron transfer. Although, RP-ISC shows high absorption of visible light and high  $\Phi_T$ , however, they are synthetically demanding, because of the large electron donor–acceptor distance.<sup>[156]</sup> Furthermore, a rigid/long linker is needed for the binding of electron donor and acceptor molecules to minimize electron coupling which may drop the electron exchange energy that is the precondition of the RP-ISC process.<sup>[157]</sup>

On other hand, direct coupling of electron donor and acceptor through C–C bond, may make an easy synthesis, showing the SOCT-ISC process by direct conversion of  $^1CT$  into  $T_1$  state.<sup>[158]</sup> The increased rigidity demonstrated a closer packing between the adjacent electron donor and acceptor molecules as shown in PXRD (Figure 5c).<sup>[159]</sup> Generally, the donor and

acceptor are directly linked to each other, adopting the orthogonal geometries for enhanced SOCT-ISC efficiency.<sup>[160]</sup> The orbital angular momentum changes during charge recombination of these electron donor-acceptor systems offset the electron spin angular momentum change during ISC, and as such, the angular momentum is conserved and ISC is enhanced.<sup>[161,162]</sup>

Various chromophores have been studied for the preparation of electron donor-acceptor dyads showing SOCT-ISC such as perylenebisimide–carbazole,<sup>[163]</sup> phenothiazine–styryl–BODIPY (PTZS–BODIPY),<sup>[164]</sup> BODIPY–anthracene,<sup>[165]</sup> and perylene–BODIPY.<sup>[166]</sup> Filatov et al.<sup>[165]</sup> for the first time developed BODIPY–anthracene dyads with  $\tau_T > 40 \mu s$  and high  $\Phi_T$  (up to 80%). Liang et al.<sup>[167]</sup> presented a comparative study using butoxy, *N,N*-dimethylaniline–BODIPY and *N,N*-imethylaniline–BODIPY chromophore to investigate their effect on SOCT-ISC efficiency. The results displayed that *N,N*-dimethylaniline, and *N,N*-dimethylaniline is stouter electron-donating moieties than butoxy with a substantial increase in SOCT-ISC and  $\tau_T = 37$ – $42 \mu s$ . In another study, perylenebisimide–carbazole dyads showed  $\tau_T = 190 \mu s$  and enhanced  $\Phi_T = 72\%$ .<sup>[163]</sup> Hou et al.<sup>[164]</sup> investigated the series of PTZS–BODIPY electron donor–acceptor dyads bestowing  $\tau_T = 303 \mu s$  which is dominantly higher in comparison with heavy atom effect molecule ( $\tau_T = 1.8 \mu s$ ).<sup>[168]</sup> Recently, Zhijia et al.<sup>[166]</sup> developed a series of perylene–BODIPY compact electron donor-acceptor dyads showing high  $\tau_T = 436 \mu s$  and  $\Phi_T = 60\%$  that is due to the efficient charge separation as shown in Figure 5d.

Irrespective of the type of donor and acceptor, there are several factors affecting  $\tau_T$ ,  $\Phi_T$  and SOCT-ISC efficacy such as, the length,<sup>[169]</sup> position,<sup>[170]</sup> and the substitution pattern<sup>[171]</sup> of chromophore linker. Similar to RP-ISC, a large length linking chromophore may lead to a decrease in electron exchange energy thus reducing the  $\Phi_T$  and  $\tau_T$ . For, example, Kepeng et al.<sup>[169]</sup> presented low  $\Phi_T = 13\%$ ,  $\tau_T = 13 \mu s$  for large linking chromophore as compared with the small chromophore linker length present high  $\Phi_T = 98\%$ ,  $\tau_T = 116$ . The position of the linkage is another important parameter contributing in  $\Phi_T$  and  $\tau_T$ , that is, the conjugation of perylenemonoimide (PTZ) with phenothiazine (PMI) at the 9–N position present reasonable restriction of conformation, and  $\tau_T = 76 \mu s$ .<sup>[172]</sup> In another study, either N— or 2—C positions of the phenothiazine—panthracene (PTZP) with BODIPY displayed efficient enhancement in SOCT-ISC.<sup>[170]</sup> Furthermore, the significant inhibition of ISC is possible with the extension of  $\pi$ -conjugation by the C≡C bond at 9,10-position.<sup>[173]</sup>

The lifetime of the TSP for PTZP–N and PTZP–C were determined as 156 and 223  $\mu s$ , respectively, which is much longer than the interaction of perylene and radical, that is RP-ISC.<sup>[174]</sup> In another study, perylenediimide–phenothiazine (PTZ–PMI) were directly connected with C–N or C–C bonds to restrain the molecular conformation and the geometry, presenting the  $\tau_T = 200 \mu s$ .<sup>[175]</sup> Solvent polarity also plays an important role to control the SOCT-ISC process. Recently, Filatov et al.<sup>[171]</sup> studied the effect of solvent polarity on the generation of triplet excited state and SOCT-ISC efficacy. The results displayed that alkyl substitution can produce a triplet excited state only in polar solvents. The twisted  $\pi$ -conjugation framework appeared to be another appealing strategy for enhanced  $\tau_T = 198 \mu s$ .<sup>[176]</sup> In another study, a significant coexistence of satisfactory  $\Phi_T = 52\%$  and long



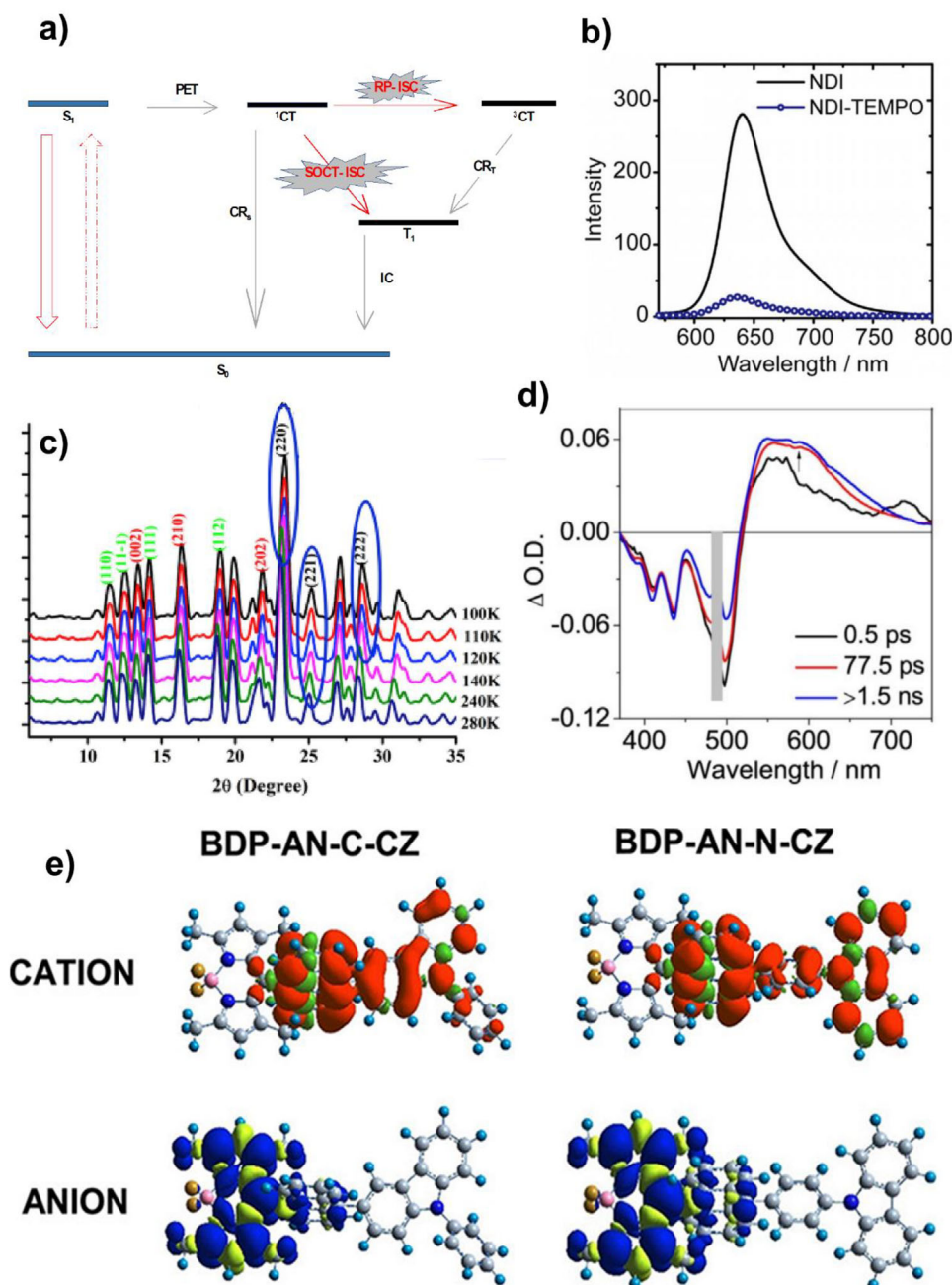


**Figure 5.** a) Jablonski diagram presenting the mechanisms of triplet state formation in electron donor-acceptor system. b) Fluorescence emission spectra of NDI and NDI-TEMPO. c) PXRD patterns of cyanyl-carboxylic derivatives at different temperatures. d) Transient absorption data of dyad BDPery-2 in toluene. e) Spin density surface distribution of the CZ-AN-BODIPY triads. b) Reproduced with permission.<sup>[155]</sup> Copyright 2018, Wiley-VCH Verlag GmbH & Co. KGaA, Weinheim. c) Reproduced with permission.<sup>[159]</sup> Copyright 2019, Elsevier Ltd. d) Reproduced with permission.<sup>[166]</sup> Copyright 2019, Wiley-VCH Verlag GmbH & Co. KGaA, Weinheim. e) Reproduced with permission.<sup>[180]</sup> Copyright 2020, American Chemical Society.

$\tau_T = 492 \mu\text{s}$  by helically twisted chromophore.<sup>[177]</sup> Dong et al.<sup>[178]</sup> studied the effect of different angle-oriented chromophores on the donor-acceptor system. The results revealed that when the angle between the donor and acceptor moiety is  $85.6^\circ$ -very close to orthogonal geometry, displayed high  $\Phi_T = 54\%$  which is twofold less when the angles reach  $49.6^\circ$  and continue to further decrease with the retardation of angle. Furthermore,  $\tau_T$  also showed a similar trend with a maximum value of  $539 \mu\text{s}$ .

Interestingly, triads have been receiving attention for enhanced SOCT-ISC efficacy and high  $\Phi_T$ . For example, Sun et al.<sup>[179]</sup> developed donor-acceptor-donor triad where donor- $\pi$ -bridge-acceptor- $\pi$ -bridge-donor is tuning the photophysical properties of the backbone. Recently, Mahmood et al.<sup>[180]</sup> developed a triad of sufficient electronic coupling by linking in a series donor-donor-acceptor such as, carbazole (CZ), anthracene (AN), and BODIPY chromophores. Interestingly, an enhancement in

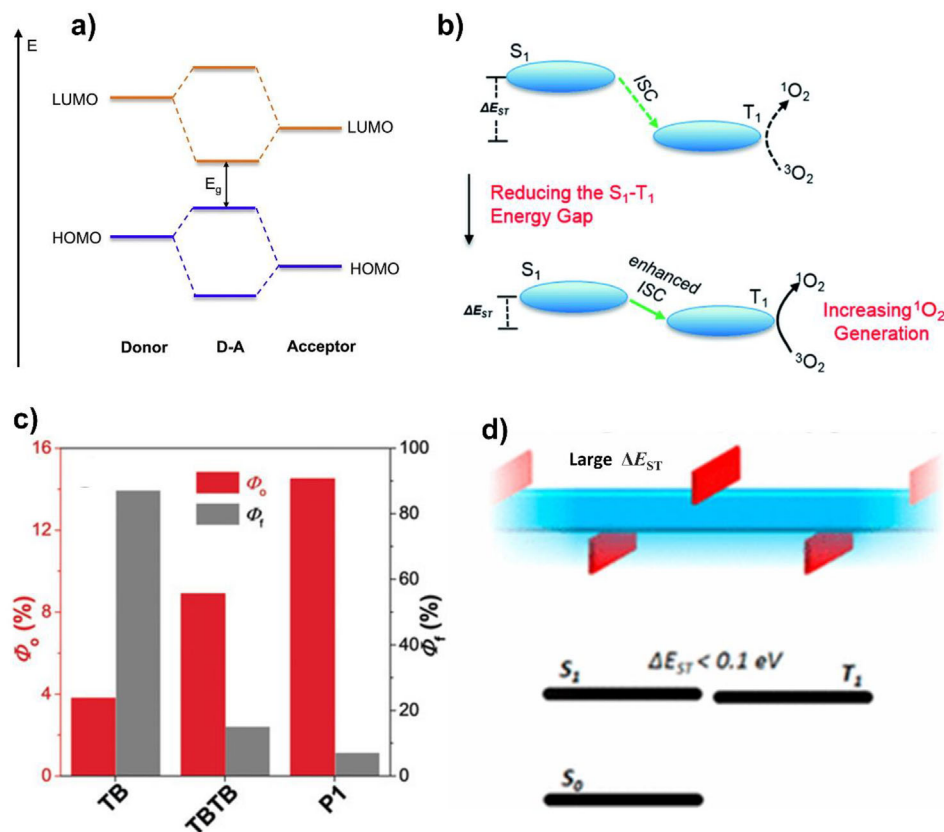


**Figure 6.** a) Schematic diagram presenting the HOMO-LUMO energy levels of donor-acceptor molecules and the molecular interaction between them. b) A physical model of  $^1O_2$  generation, representing the  $S_1$ - $T_1$  ISC method and the proposed tactic for improving  $^1O_2$  generation. c)  $\Phi_\Delta$  and fluorescence of TB (donor-acceptor), TBTB (donor-acceptor-donor-acceptor) and P1 (polymer). d) The schematics of the donor (blue) and an orthogonal acceptor (red) conjugation and their perspective singlet-triplet energy gap. a) Reproduced with permission.<sup>[185]</sup> Copyright 2017, Elsevier B.V. b) Reproduced with permission.<sup>[186]</sup> Copyright 2015, The Royal Society Of Chemistry. c) Reproduced with permission.<sup>[189]</sup> Copyright 2018, Wiley-VCH Verlag GmbH & Co. KGaA, Weinheim. d) Reproduced with permission.<sup>[191]</sup> Copyright 2017, American Chemical Society.

SOCT-ISC efficacy has been observed as compared with the AN-BODIPY dyad. Furthermore, the contribution of electron donor and acceptor moieties was confirmed through the spin density surface distribution of radical cations and anions as shown in Figure 5e suggesting the confinement of holes on the AN and CZ while the electrons were localized on BODIPY. Moreover, the equal contribution of AN and CZ proposing that both electron donor moieties take part in the photoinduced electron transfer process by the sequential electron transfer process.

### 3.3. Reducing the Singlet-Triplet Energy Gap

TSP concentration quenching is another challenging prospective that shortens the efficacy of PSs to generate  $^1O_2$ . The quenching effect is particularly more common in hydrophobic PSs due to their aggregation properties in aqueous media.<sup>[181]</sup>

Several strategies have been developed to reduce  $\Delta E_{ST}$  including the electron donor-acceptor system<sup>[182,183]</sup> and  $\pi$ - $\pi$  stacking.<sup>[184]</sup>

Generally, a material of electron donor-acceptor system demonstrate low  $\Delta E_{ST}$ , if the highest occupied molecular orbital (HOMO) of the donor atom and the lowest unoccupied molec-

ular orbital (LUMO) of an acceptor atom are available at a similar energy level (Figure 6a).<sup>[185]</sup> Thus, a significant overlap between HOMO of donor atom and LUMO of acceptor atom can be custom made to tune the  $\Delta E_{ST}$  (generally,  $\Delta E_{ST} < 0.2$  eV), enabling most of the  $S_1$  exciton transfer to  $T_1$  state to achieve enhanced ISC, high  $\Phi_\Delta$  (Figure 6b)<sup>[186]</sup> and improved PDT efficacy<sup>[56,183]</sup> with an easy energy conversion between singlet and triplet PSs.<sup>[187]</sup> Shao et al.<sup>[181]</sup> introduced two thiophene rings into the backbone of isoindigo donor and triphenylamine acceptor atoms to facilitate fast intramolecular charge transfer, enhanced  $\Phi_\Delta$  (84.0%), and narrowed  $\Delta E_{ST}$  of 0.65 eV. In another study, Musib et al.<sup>[188]</sup> has been developed a curcumin-based lanthanide (La) complex to combine excellent photosensitizing properties of curcumin. La is responsible for enhanced ISC of curcumin and improved  $\tau_T$  which leads to higher  $\Phi_\Delta$ .

Furthermore, the increasing polymerization,<sup>[189]</sup> twisted conformation,<sup>[183,189]</sup> and ligand orientation<sup>[190]</sup> are also effective techniques to reduce  $\Delta E_{ST}$ , enhance  $\Phi_\Delta$  and reduce fluorescence. For example, demonstrated reduce  $\Delta E_{ST}$ , enhance  $\Phi_\Delta$  and reduce fluorescence with enhanced polymerization of donor-acceptor, as shown in Figure 5c.<sup>[189]</sup> Twisted conformation of the donor-acceptor system also showed beneficially reduced  $\Delta E_{ST}$  and improved ISC.<sup>[183,189]</sup> Recently, Leitel et al.<sup>[190]</sup> presented

a much higher  $\Delta E_{ST} = 3700 \text{ cm}^{-1}$  at an optimized torsion angle of  $70^\circ$  as compared with  $\Delta E_{ST} = 740 \text{ cm}^{-1}$  at  $5^\circ$ . In another study, Freeman et al.<sup>[191]</sup> attained a reduced  $\Delta E_{ST}$  by conjugating the donor atom with an orthogonal acceptor atom which facilitated the spatial overlap of frontier molecular orbitals as shown in Figure 6d.<sup>[191]</sup>

Interestingly, a recent development in the research area of light-emitting diodes using thermally activated delayed fluorescence (TADF) emitters with exceptionally small  $\Delta E_{ST}$  (0.01–0.05 eV) values<sup>[192,193]</sup> opened up the doors to prepare metal-free small  $\Delta E_{ST}$  PSs with enhanced ISC<sup>[194]</sup> and high  $\Phi_T$ .<sup>[195]</sup> Generally, TADF generation appear with in the charge transfer system having thermally accessible gap in between the S1 and T1 states<sup>[196,197]</sup> and it also requires appropriate placement of donor and acceptor molecules to minimize HOMO-LUMO overlap, for enhanced emission efficiency and lower  $\Delta E_{ST}$  values.<sup>[198]</sup> For example, Woo et al.<sup>[199]</sup> prepared a spiro-silicon-connected silafluorene–phenazasiline donor by integrating triphenyltriazine as an acceptor to achieve  $\Delta E_{ST}$  of 0.2 eV. Uoyama et al.<sup>[200]</sup> prepared a twisted donor-acceptor system by introducing steric hindrance through bulky substitution which leads to enhanced TADF and a small  $\Delta E_{ST}$  of 0.11 eV. In another study, Jinfeng et al.<sup>[201]</sup> developed two-photon activated TADF nanoparticles to achieve enhanced PDT ( $\Phi_\Delta = 52\%$ ) owing to a small  $\Delta E_{ST}$  of 0.23 eV. Furthermore,  $\Delta E_{ST}$  values of TADF materials can be much reduced with enhanced solvent polarity by doping TADF materials with a polar matrix.<sup>[202]</sup> In another study, Haseyama et al.<sup>[203]</sup> presented reduced  $\Delta E_{ST}$  values of TADF with the conjugation of the polar inert molecule.

Although the donor-acceptor system effectively reduced the  $\Delta E_{ST}$  values by lowering the S1 up to 0.1 eV T1, with barely changing the energy level of T1, thus leading to fast triplet recombination. In this context,  $\pi$ – $\pi$  stacking is found to be an effective strategy for sufficiently reduced  $\Delta E_{ST}$  and enhanced absorption.<sup>[184]</sup> For example, the conjugation of naphthalene units in the rylene diimide dyes turned over the  $\Delta E_{ST}$  from 1.29 to 2.15 eV.<sup>[204]</sup> However, the reduction in  $\Delta E_{ST}$  is highly dependent on the chain length of the  $\pi$ – $\pi$  stacking group.<sup>[205,206]</sup> Furthermore, the  $\pi$ – $\pi$  stacking materials with large density values have been considered tremendous attention to self-assemble and cross-link 3D networks.<sup>[207]</sup> Moreover, the geometry of the interaction of  $\pi$ – $\pi$  stacking also showed a contribution. Several investigations have confirmed that offset stacked and edge-to-face stacked are energetically superior when comparing with face-to-surface stacking.<sup>[208]</sup>

#### 4. Advances in Nanocarriers

Advances in nanotechnology have opened up new horizons in the application of PSs in PDT. To enable PDT to be more widely used in the field of cancer therapy, higher demand has been placed on the delivery system of PSs. The following are some of the PSs based systems which have been significantly improved to enhance the efficacy of PDT. First, the drug delivery system targeting cancer cells has been re-designed, which can significantly reduce the side effects of PDT. Second, the delivery system of PSs targeting specific organelles has also been re-designed to improve the lethality against cancer cells. Last but not least, the synthesis of many new PSs has been improved.

#### 4.1. Cancer Cells Targeting in General

Although compared with other traditional therapies, PDT has shown its excellent advantages in reducing side effects, persistent skin photosensitization is still one of the limiting factors for its clinical promotion. Therefore, it is particularly important to target tumors and improve the enrichment rate of PSs in cancer cells in order to solve the above problems. Tumor targeting strategies can be divided into active and passive.

Generally, high-affinity ligands can be used to improve tumor targeting, including ligands that target tumor cells and ligands that target the tumor microenvironment (TME). Active targeting is used by modified drug carriers to transport drugs into the target area for concentration. Because the surface of drug-loaded particles is connected with specific ligands that can bind to the receptors of target cells, it can change the natural distribution of drugs in vivo.<sup>[209]</sup> With the development of gene sequencing and proteomics, many biomaterials over-expressed in cancer cells have been detected.<sup>[210]</sup> Some of them are well suited as active targeting receptors, such as folic acid (FA) and transferrin (TF).<sup>[211]</sup> Besides, cancer stem cells (CSCs), as a subset of tumor cells with the function of self-renewal and differentiation, have also attracted attention. The most common CSCs surface markers include CD24, CD34, CD44, CD133, ALDH1A1, and epithelial cell adhesion molecules. Among them, the overexpression of CD44 and CD133 has been reported in different types of cancers and is closely associated with patient prognosis, therefore, these two antigens may serve as ideal targeting receptors. Guan et al.<sup>[212]</sup> reported a nanoscale covalent organic framework-based nano agent, which is surface-decorated with glycosaminoglycan as a targeting agent for CD44 receptors on digestive tract tumor cells. This nano-drug delivery system can not only selectively target gastrointestinal tumor cells, but also realize the combination of calcium overload therapy and PDT, which greatly improves the killing effect on the gastrointestinal tumor. Similarly, Yan et al.<sup>[213]</sup> synthesized a novel PSs, CD133-pyro, by conjugating pyropheophorbide-a (pyro) with the peptide domain targeting CD133, and achieved the targeting of colon cancer cells in mouse models. In addition, some tumor cells have their specific expression antibodies, which can also be used as targets. For example, PSMA-targeted melanin-like nanoparticles can be used as a multifunctional nanoplatform for prostate cancer theranostics.<sup>[214]</sup>

In addition to the specific antibodies highly expressed on the surface of these tumor cells, the disordered function and structure in the whole tumor environment are also significantly different from those in normal tissues. The substitutes of the TME including dendritic cells, tumor vasculature, and hypoxic state, etc., all of these can be used as potential targets of PDT. As one of the characteristics of TME, disordered proliferative vessels can be specifically targeted by the dendrimer-fucoidan polyionic nanocomplex. Based on this, Chung et al. Developed a biocompatible therapeutic nano platform to improve the targeting of drugs to tumor: (FM@VP).<sup>[215]</sup> They used verteporfin (VP) as PSs, to co-assemble with MnO nanoparticles (a TME responsive oxygen-evolving nanomaterial) modified with a functional polysaccharide fucoidan and a bioreducible polyamidoamine dendrimer. This nano platform can not only target the TME but also effectively overcome tumor hypoxia, which has a good clinical application prospect. Hypoxia, as another significant feature

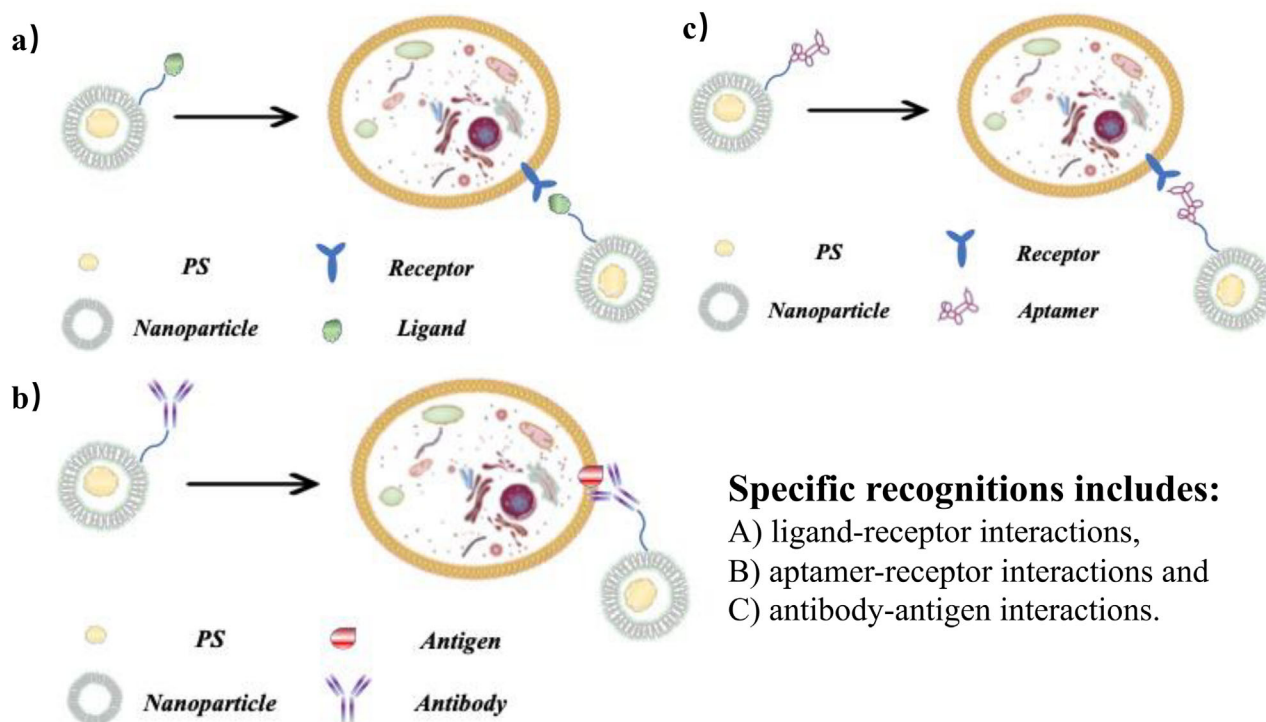


**Figure 7.** Classical model of active targeted therapy of PDT.

### Specific recognitions includes:

- A) ligand-receptor interactions,
- B) aptamer-receptor interactions and
- C) antibody-antigen interactions.

of the TME, is also worthy of good use. Based on calixarene, Zhang et al.<sup>[216]</sup> designed a hypoxia-responsive molecular container named CAC4A. This drug delivery system can load a variety of clinical drugs, including PS, and improve their biocompatibility and stability. Moreover, the azo functional groups on CAC4A can be sensitive to hypoxia, to achieve the tumor-targeting function. In general, the development of this new drug delivery platform is a major breakthrough in the field of hypoxia administration.

Passive targeting can be achieved by adjusting the physical and chemical properties of nanoparticles, such as size, morphology, structure, and surface properties, so that they can enter specific targets independent of the recognition ability of targeted molecules.<sup>[217]</sup> In addition, the EPR (enhanced permeability and retention) effect of tumor also promotes the realization of the passive target. The mechanism of the EPR effect is as follows: because the growth rate of tumor is significantly higher than that of normal tissue, there are defects between tumor vascular endothelial cells, the arrangement is not tight, and the lymphatic drainage in the tumor is insufficient, the blood flow rate is low, once the nanoparticles enter, they will be detained in the tumor site.<sup>[218]</sup> In addition to the well-known theory of EPR, recently, Warren C. W. Chan's team proved that the transport of nanoparticles through the intercellular gap of tumor vascular endothelial cells is the main reason for the passive high aggregation of nanoparticles in tumor cells.<sup>[219]</sup> This subverts the traditional perception of the passive targeting ability of nanoparticles. Although the details of the mechanism of endocytosis need to be clarified, many experimental and clinical data have proved that nanoparticles with a size of 10–200 nm can show a significant passive targeting effect.

Zhang et al.<sup>[220]</sup> designed a kind of HA-BP nanoparticles modified by pegylated hyaluronic acid (HA) for PDT. Fluorescence and photoacoustic multi-functional imaging proved that HA-BP was selectively accumulated in the tumor site due to the passive EPR effect. Similarly, Yang et al.<sup>[221]</sup> dissolved oil-soluble bimetallic metal nanoclusters into the hydrophobic cavity of biodegradable amphiphilic chitosan derivative micelles to form nanoparticles with a size of about 60 nm. This also effectively realizes the passive targeted delivery. The aforementioned strategies can facilitate the accumulation of PDT agents in the extracellular matrix of tumor tissues, reduce the overall drug delivery requirements and the side effects. **Figure 7** shows the classic model of active-targeted therapy of PDT.

#### 4.2. Organelle Targeting in Cells

Because of the short lifetime of  $^1\text{O}_2$  (about 200 ns) produced by PDT in cells, and the limitation of the diffusion distance (about 50 nm) among TME, only the organelles close to  $^1\text{O}_2$  will receive oxidative damage.<sup>[222]</sup> Therefore, the localization of PSs in important subcellular organelles such as the nucleus, mitochondria, and endoplasmic reticulum can enhance the phototoxicity of  $^1\text{O}_2$  and enhance the efficacy of PDT.<sup>[223,224]</sup>

Deng et al.<sup>[225]</sup> developed PSs for targeting the endoplasmic reticulum. The PSs can accumulate in the endoplasmic reticulum and produce ROS such as  $^1\text{O}_2$  species under light conditions, causing endoplasmic reticulum stress (ERS). ERS can induce immunogenic cell death (ICD), which greatly reduces the recurrence rate of tumors after treatment (**Figure 8**). In addition,

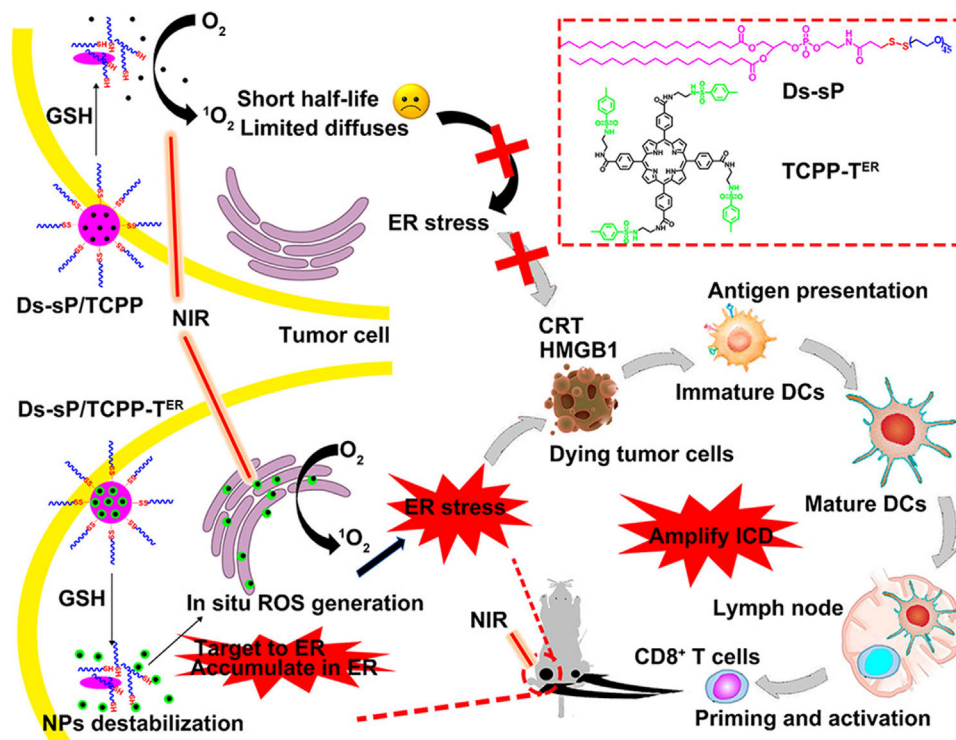


**Figure 8.** Schematics presentation of immunogenic cell death induced with endoplasmic reticulum stress. Reproduced with permission.<sup>[225]</sup> Copyright 2020, American Chemical Society.

the development of triphenylphosphine ligands has achieved mitochondrial targeting.<sup>[226–228]</sup> PSs equipped with this ligand can produce excellent phototoxicity to tumor cells under light conditions. Liu et al. reported pre-PSs based on redox activation: aPS.<sup>[229]</sup> aPS can react with glutathione and hydrogen peroxide, which are highly expressed in TME, and convert into PS efficiently. What is more, its surface is modified with triphenylphosphine ligand targeting mitochondria, which plays a specific cytotoxic effect on mitochondria in cancer cells. This makes the drug still have good phototoxicity even in the condition of hypoxia. In another study, Wang et al.<sup>[230]</sup> designed new PSs targeting mitochondria, which were encapsulated with natural low-density lipoprotein (LDL) to kill cancer cells overexpressing LDL receptors. Recently, Qiao et al.<sup>[231]</sup> developed a conjugate named Ru(II)—BODIPY. The polymer can not only produce strong phototoxicity in the range of NIR but also achieve lysosomal targeting in cancer cells. Cell experiments showed that it had a more efficient PDT effect on malignant melanoma A375 cells ( $\text{pi} = 3448$ ) and A375 mouse xenograft.

### 4.3. Localized Delivery of Photosensitizer

Due to the short lifetime of  $^1\text{O}_2$ , their reactivity with biological molecules is limited in nearby regions. Thus PSs localization is needed to enhance targeted sensitization, enhanced  $\Phi_{\Delta}$ , and improved PDT efficacy. The PSs with dissimilar pharmacokinetics showed a difference in tumor localization properties.<sup>[232]</sup> Generally, the PSs of fast pharmacokinetics revealed high accumulation due to the increased permeability in tumor neovasculature.<sup>[233]</sup>

While the localization with slow pharmacokinetics is attributed to the distinctive properties of tumor cells when comparing with normal tissue such as poorly developed lymphatic drainage, the overexpressed LDL, low pH value, and tumor-associated macrophages.<sup>[234]</sup>

To enhance the PS accumulation rate, various nanocarriers have been developed such as, liposomes and micelles,<sup>[59,235]</sup> polymer nanoparticles,<sup>[60,236,237]</sup> and graphene oxide (GO).<sup>[61]</sup> Liposomes and micelles were the first nanocarriers investigated for the delivery of PSs in PDT.<sup>[238]</sup> Although both liposomes and micelles showed similar structures with some differences in their structure and chemical composition. Micelles are generally monolayer structures composed of the block copolymer or amphiphilic molecules in colloidal dispersions, where the pyrophosphoric tails directed toward the center and hydrophilic heads are in contact with the aqueous phase, that is, the liquid suspension.<sup>[239]</sup> Thus, they are able to carry hydrophobic PSs molecules which can covalently or physically bond with the hydrophobic core.<sup>[59]</sup> Micelles have been widely studied but the limitation of their practical applications is the prolonged photosensitivity.<sup>[239]</sup>

A liposome is composed of lipid bilayers, entrapping the hydrophobic PSs within the bilayer or hydrophilic PSs within the central aqueous core compartment.<sup>[235]</sup> Liposomes showed high biocompatibility, high stability in the biological environment, and controlled release.<sup>[240]</sup> Despite the success in the development of liposomes, their performance was limited due to their unprotected surface which leads to a reduction in surface tension and aggregation of serum protein.<sup>[241]</sup> In this regard, coating techniques have been developed for surface modification.<sup>[242–244]</sup>

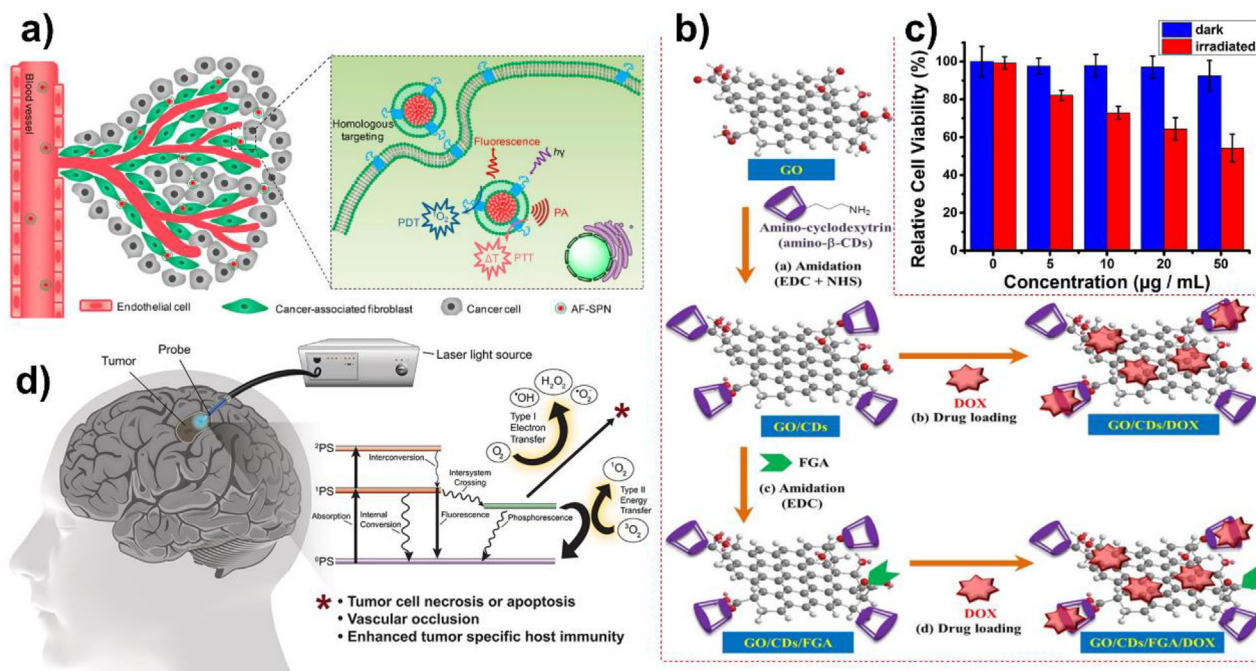


**Figure 9.** a) Schematic diagram presenting the targeting of AF-SPN to cancer-associated fibroblasts in tumor tissues. b) Synthesis schematics of GO composites. c) Cell viabilities of UMUC3 cells, blue for dark treatment, red for light irradiation, Note: PEG nano GO PSs solution incubation concentration: 0, 5, 10, 20, and 50  $\mu\text{g mL}^{-1}$ . d) Pictorial representation of wireless photonic PDT of glioblastoma. a) Reproduced with permission.<sup>[236]</sup> Copyright 2018, American Chemical Society. b) Reproduced with permission.<sup>[61]</sup> Copyright 2018, Elsevier B.V. c) Reproduced with permission.<sup>[256]</sup> Copyright 2018, American Chemical Society. d) Reproduced according to the terms of the CC-BY license.<sup>[258]</sup> Copyright 2020, The Authors.

Among them, polyethylene glycol (PEG) is the broadly used polymer for liposome stabilization.<sup>[245,246]</sup> with a slow fusion rate and inhibited protein adsorption, thus providing enhanced in vivo circulation time.<sup>[247–249]</sup>

Polymeric nanoparticles are classified as nanospheres and nanocapsules.<sup>[238]</sup> The nanocapsules are core-shell systems formed hydrophilic or lipophilic core and a polymeric shell. In contrast, nanospheres consist of a solid polymeric structure entrapping the PSs molecule. Hu et al.<sup>[60]</sup> developed paclitaxel with poly( $\epsilon$ -caprolactone-*co*-lactide)-*b*-poly(ethylene glycol)-*b*-poly( $\epsilon$ -caprolactone-*co*-lactide) copolymer by ring-opening polymerization in the presence of PEG. The developed polymer-based nanoparticles showed efficient passive tumor accumulation. In another study, Li et al.<sup>[236]</sup> developed a poly(cyclopentadithiophene-*alt*-benzothiadiazole) polymer coated with the cell membranes of activated fibroblasts (AF-SPN) for selective targeting of fibroblast associated with cancer with enhanced accumulation as shown in **Figure 9a**. In another study, PpIX-loaded hyaluronic acid-*b*-poly(d,l-lactide-*co*-glycolide) copolymer was developed to treat CD44-overexpressing cancers. The developed hybrid polymer-based nanoparticles showed dose-dependent cytotoxicity.<sup>[250]</sup> The nanoparticle's synthesis, composition, and design can be easily controlled to tune size, surface properties, and shape.<sup>[251]</sup> In particular, biocompatible coatings such as chitosan, polypeptide, and albumin help to improve biocompatibility.<sup>[252]</sup>

Carbon base materials such as GO are considered tremendous attention due to their high surface area and high drug loading capacity.<sup>[253]</sup> Miao et al.<sup>[254]</sup> observed that PSs chlorin e6 (Ce6)

loaded PEG-GO nanosheets showed higher tumor accumulation as compared with uncoated Ce6 PSs due to enhanced permeability and retention in tumor tissues. In another study folic acid has been introduced into the GO nanocarrier of Ce6 PSs for specific targeting of cells with folate receptors.<sup>[255]</sup> Siviriyannun et al.<sup>[61]</sup> prepared a composite of GO using  $\beta$ -cyclodextrin (CD) and poly(amidoamine) dendrimer (DEN) by covalent bonding which followed with amide formation using two condensing agents named N-hydroxysuccinimide (NHS), 1-[3-(dimethylamino)propyl]-3-ethylcarbodiimide hydrochloride (EDC), as shown in **Figure 9b**. The developed composite showed a significant cellular uptake of 99.95 by HeLa cells. In another study, Sun et al.<sup>[256]</sup> investigated the cytotoxicity of PEG-nano GO PSs on UMUC3 cells. **Figure 9c** showed the low cytotoxicity of PEG nano GO PSs, witnessed with high relative cell viability of higher than 90% at 50  $\mu\text{g mL}^{-1}$ .

Recently, fiber optic technology is appearing as an attractive technology with focused irradiation, leading to a high dosage of light and decreased photocytotoxicity in non-targeted regions.<sup>[257]</sup> Thus, fiber optic technology guarantees high effectiveness with low damage to neighboring cells.<sup>[62]</sup> In another study,<sup>[258]</sup> employed interstitial PDT through fiber optic capable (**Figure 9d**) to provide photostimulation after the delivery of PSs to treat a series of 350 patients with glioblastoma and summarized the overall survival rates for the newly diagnosed patients. Bartusik et al.<sup>[259]</sup> have established a portable fiber optic-based PSs delivery system that was used to evaluate the  $\Phi_{\Delta}$  within the local vicinity in vitro in ovarian cancer cells. The fiber optic system was made of mesoporous fluorinated silica tip and

a photo-cleavable linker was used to bind the PSs molecules onto it. At the same, molecular oxygen was also administrated through the fiber optic to facilitate much enhanced  $^1\text{O}_2$  production. Kang et al.<sup>[260]</sup> developed mitochondrial-targeted PSs (4-carboxy-butyl)-triphenyl phosphonium-pheophorbide-a (TPP-PheoA) conjugate-loaded albumin nanoparticles (PS@chol-BSA NPs) molecules. The performance of developed PSs was further enhanced by using a fiber-optic cannula in orthotopic GBM-xenografted mice. Bansal et al.<sup>[261]</sup> demonstrated the clinical PDT using an optical fiber for wireless photonic approaches, which allows on-demand light activation of PSs deep in the body. Recently, Kustove et al.<sup>[262]</sup> developed a single fiber system for both transmitting the laser irradiation and receiving the fluorescent signal.

## 5. The Immune Response Induced by $^1\text{O}_2$

Several studies have shown that  $^1\text{O}_2$  can effectively regulate innate immunity and adaptive immunity. On the one hand, local injuries and oxidative stress activate an acute inflammatory process but on the other hand, ICD induced by  $^1\text{O}_2$  can activate the adaptive immune response of the human body by releasing damage-associated molecular patterns (DAMPs).

### 5.1. Innate Immunity Induced by $^1\text{O}_2$

Innate immunity, also known as non-specific immunity, refers to the body's innate normal physiological defense function, which can make a corresponding immune response to the invasion of various pathogenic microorganisms and foreign bodies. Both apoptotic and necrotic tumor cells promoted by  $^1\text{O}_2$  can activate the immune system and induce the immune response. After the death and lysis of tumor cells, the cell debris or various cytosolic components produced will cause a strong inflammatory reaction in the surrounding tissues. Various cells in TME, such as surviving tumor cells, damaged endothelial cells, tumor stromal cells, etc., can release a large number of inflammatory promoting media, including arachidonic acid, cytokines, histamine, and complement system.<sup>[263]</sup> These components enhance the chemotaxis, activation, and phagocytosis of macrophages, and make neutrophils aggregate, resulting in tumor-specific primary and memory CD8 (+) T cell responses. For example, Yamamoto et al.<sup>[264]</sup> described a macrophage activation (innate immune activation) mediated by Fc receptor because of the peroxidation of lipid membrane caused by  $^1\text{O}_2$  during PDT. After macrophages phagocytize the dead cancer cells and present antigens, the adaptive immunity dominated by lymphocytes will be activated accordingly. A variety of lymphokines secreted by lymphocytes can further enhance the ability of innate immunity to kill target cells. Moreover, neutrophil infiltration in tumor area can promote the proliferation and survival of T cells, which provides important support for the establishment of anti-tumor immunity.<sup>[265]</sup>

### 5.2. Adaptive Immunity Induced by $^1\text{O}_2$

Besides killing tumor cells directly, ICD is a more important phenomenon mediated by  $^1\text{O}_2$ , which may become the most promis-

ing ways to achieve total tumor cell elimination. ICD can increase the immunogenicity of TME by releasing DAMPs and then activate T cell adaptive immune response to form long-term immune memory.<sup>[266–269]</sup> ICD needs to be achieved by stimulating cells to produce ERS, a response process in which cells activate unfolded protein response, endoplasmic reticulum overload response, and caspase-12-mediated apoptosis pathway in response to the external stimulus.  $^1\text{O}_2$  can trigger ER stress and induce downstream DAMPs/DANGER signaling pathway,<sup>[270]</sup> which will more effectively promote the release of DAMPs such as calcium reticulin.<sup>[271]</sup> Generally, DAMPs belong to the normal components of cells and participate in their physiological activities, but when these substances are secreted out of cells (cell death or stimulation), they evolve into dangerous signals in the human body and further amplify the immune function.<sup>[75]</sup> First, DAMPs can induce the maturation of dendritic cells (DCs). These mature DC cells can present cancer cell antigen to primitive T cells and promote their differentiation into effector T cells (CT8).<sup>[272]</sup> Then, DAMPs will simultaneously recruit antigen-presenting cells (APCs) other than DC cells and promote their maturation. These APCs can present tumor-associated antigen and new tumor antigen to effector T cells, further increasing the anti-tumor effect of T cells (**Figure 10**). At present, the study of extracellular heat-shock protein 70 (HSP70) is the most in-depth, and it is also considered to be one of the most important DAMPs. In cells, HSP70 plays an important role in inhibiting protein aggregation and inhibiting apoptosis.<sup>[273]</sup> However, when cells are exposed to ERS and HSP70 is released to the outside of cells, it can promote the maturation of DC cells and specifically bind to high-affinity receptors on the surface of APCs to start the ICD program. In addition to the heat shock protein family, more and more DAMPs have been found and further studied, such as, high-mobility group box 1, ATP, annexin A1, type I interferons, and mitochondrial DNA.<sup>[268,274,275]</sup> The various DAMPs described above are distinguished in their cellular function, localization, etc. The manner of their release, and the mechanisms by which they trigger ICD are also different.

In conclusion,  $^1\text{O}_2$  can mediate ICD, which enables the effective eradication of primary tumors. At the same time, DAMPs released by  $^1\text{O}_2$  can stimulate the immune response and enhance the inherent weak immune stimulation characteristics of natural tumor antigen.<sup>[276]</sup>

## 6. Synergetic Therapy of Photodynamic Therapy

A reasonable combination of drugs with different anti-tumor mechanisms can not only improve the curative effect, reduce the drug resistance of tumor, but also reduce the side effects caused by the dose problem. Based on this principle, the unique phototoxicity and noninvasiveness of  $^1\text{O}_2$  make PDT a popular choice for combination therapy.<sup>[17]</sup> On the one hand, the combined therapy strategy can make up for the defect that PDT cannot completely cure solid tumors alone. On the other hand, combined with appropriate traditional therapy, the dose requirement of PS can be reduced under the premise of the same therapeutic effect, and the phototoxicity of PDT to human non-malignant tissues can be minimized (**Figure 11**).

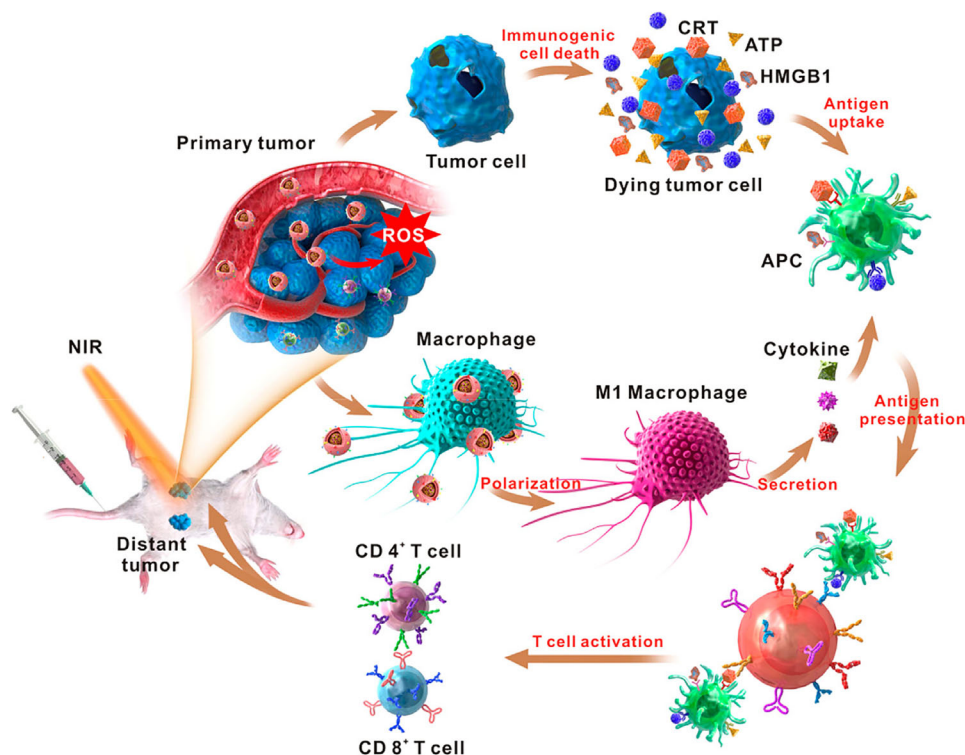


**Figure 10.** Mechanism of ICD activation after PDT treatment. The debris released by the dead tumor cells is directly or indirectly absorbed by APCs, activating the mature differentiation of T cells, and causing secondary killing to the surviving tumor cells. Reproduced with permission.<sup>[277]</sup> Copyright 2018, American Chemical Society.

### 6.1. Combined Photodynamic Therapy and Photothermal Therapy

PDT and photothermal therapy (PTT) both use light to stimulate cytotoxic effects to kill the tumor, and they have a potential synergistic effect. Therefore, the combination of PDT and PTT will play a role of one plus one greater than two. On the one hand, the thermodynamic effect of PTT can improve the local blood flow and increase the oxygen concentration in the tumor tissue, resulting in higher PDT efficacy.<sup>[282,283]</sup> On the other hand, ROS produced between PDT can destroy heat shock proteins, thus reducing their protective effect on tumor cells during PTT.<sup>[284]</sup>

Nano covalent organic frameworks are a new kind of porous materials suitable for carrying PSs and photothermal agents at the same time. Guan et al.<sup>[278]</sup> successfully prepared a dual-mode PDT/PTT nano-drug delivery system by using step-by-step bond defect functionalization. This nano platform not only connects porphyrin as PSs but also noncovalently loads naphthalene phthalocyanine as a photothermal agent. It realizes the combination therapy of PTT and PDT and has a significant effect on inhibiting tumor growth and metastasis. In another study, Yang et al.<sup>[285]</sup> used hollow nitrogen-doped carbon nanospheres (HNCS) and iron phthalocyanine (FePc) to construct a nanoenzyme mediated cooperative dual phototherapy nanoplatform: FePc/HNCS. The newly constructed nano platform not only successfully combines PDT with PTT but also reduces hypoxia limitation by catalyzing endogenous hydrogen peroxide, achieving a high tumor inhibition rate of 96.3%. Although the combination therapy of PDT and

PTT shows good therapeutic potential, there are still some problems hindering its wide application. Due to the commonly mismatched absorption spectra of photothermal agents and photodynamic agents, combined PTT and PDT require sequential tumor irradiation using two different lasers, which prolongs treatment times and complicates the treatment process. Besides, the proportion of PSs and photothermal agents, whether they will affect each other, and the order of laser irradiation are also issued to be considered. In order to solve these problems, scientists have made many research and attempts. They found that Au nanovesicles and Au nanostars loaded PSs CE6 can be used to enhance PDT/PTT, which can realize the synchronization of PDT and PTT under single laser irradiation.<sup>[286,287]</sup> On this basis, inspired by the bimolecular structure of cell membrane phospholipids, Liu et al.<sup>[288]</sup> constructed a biomimetic cell membrane polymeric vesicle by using the coordination of cetyltrimethylammonium bromide on the surface of hydrophobic gold nanorods (AuNRs) with indocyanine green (ICG) and polycaprolactone, which realized the synergistic effect of PDT/PTT in the treatment of prostate cancer. Recently, Li et al.<sup>[289]</sup> designed and synthesized a small molecule with a “receptor donor receptor” structure. This multifunctional molecule not only realizes the combined therapy of PDT and PTT but also has the function of multimodal imaging. The experimental data show that the generation of reactive oxygen is 3.2 times higher than that of ICG and the photothermal conversion efficiency is 52.8%.

The combined application of PDT and PTT has increased the lethality of single irradiation to tumor several times. However,



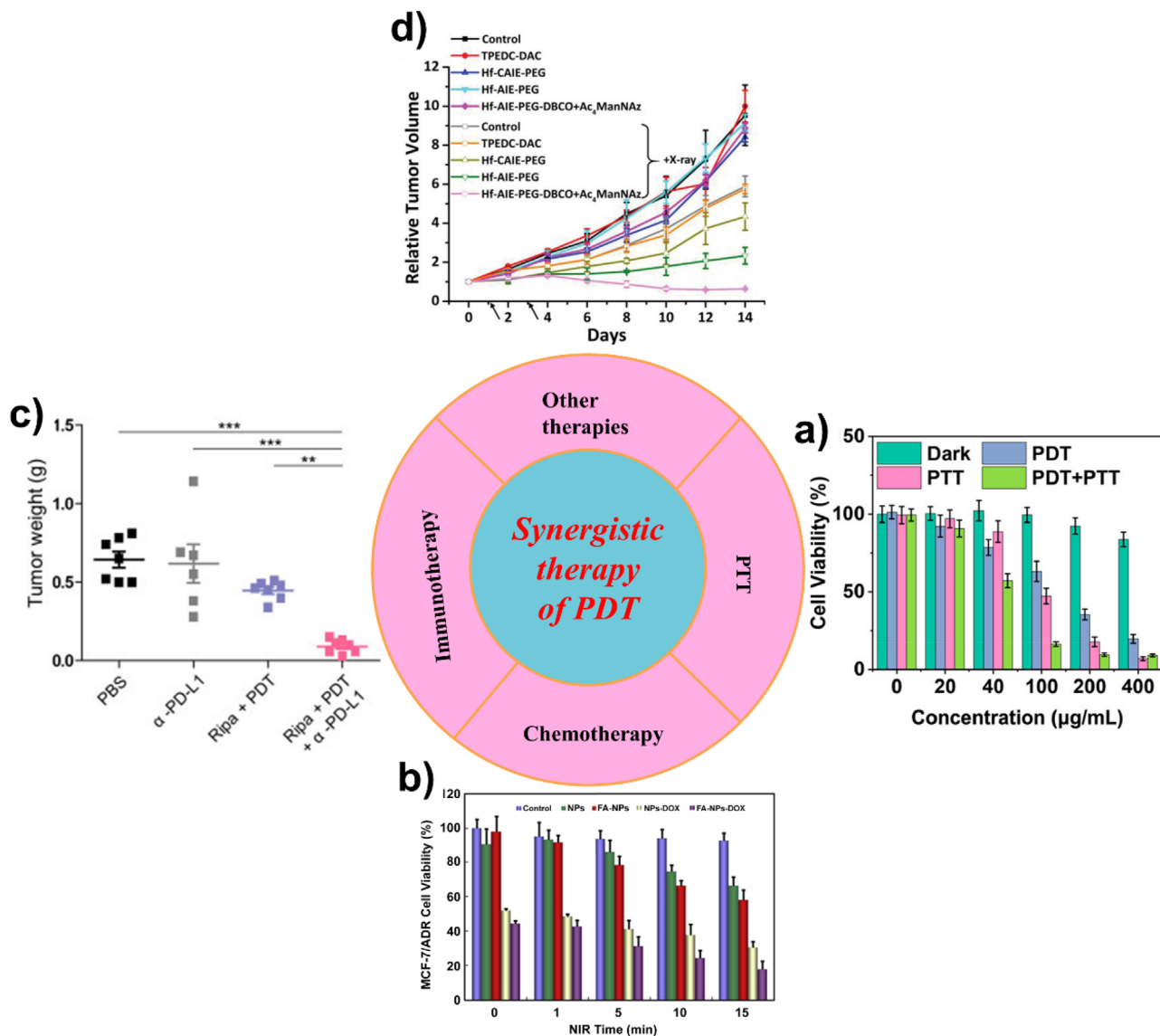


**Figure 11.** Schematic representation of several strategies that can be combined with PDT for better cytotoxicity and efficacy, a) PDT and PTT, b) PDT and chemotherapy, c) PDT and immunotherapy, and d) PDT and other therapies. a) Reproduced with permission.<sup>[278]</sup> Copyright 2019, American Chemical Society. b) Reproduced with permission.<sup>[279]</sup> Copyright 2015, Elsevier Ltd. c) Reproduced with permission.<sup>[280]</sup> Copyright 2021, The Authors. d) Reproduced with permission.<sup>[281]</sup> Copyright 2021, Wiley-VCH GmbH.

so far, almost all studies have shown that this treatment mode cannot effectively prevent the growth of distant metastatic tumor tissue. It makes patients have long-term complications of tumor recurrence, which is not conducive to the prognosis of patients. In addition, as an ideal photosensitizer that can activate PTT and PDT at the same time, heavy metal nanoparticles will accumulate in human tissues for a long time. Its safety and toxicity profiles are still problematic.

## 6.2. Combined Photodynamic Therapy and Chemotherapy

The combination of PSs and chemo-drugs may produce synergistic PDT/chemotherapy therapeutic effects, in which chemother-

apy can solve the limitation of PDT to a certain extent, while PDT, in turn, suppresses the drug-efflux activity of cells and enhances the cellular uptake of drugs. Specifically, chemotherapy can disregard the limitation of light penetration in PDT and can also improve the sensitivity of cancer cells to <sup>1</sup>O<sub>2</sub> generated in PDT.<sup>[290,291]</sup> Meanwhile, PSs can inhibit P-glycoprotein pumps (PGP) to reduce drug efflux from tumor cells,<sup>[292]</sup> and solve the problem of multi-drug resistance (MDR) to a certain extent. MDR refers to the cross-resistance of tumor cells to some chemotherapeutic drugs and other antitumor drugs with different mechanisms. The main mechanism of MDR resistance is the amplification of the MDR1 gene and the overexpression of PGP. As an ATP-dependent drug delivery pump, PGP can actively pump hydrophobic anti-tumor drugs out of the cell, thus reducing

intracellular drug accumulation and increasing drug efflux. MDR, the most leading cause of chemotherapy failure, seriously affects the prognosis of cancer patients. Fortunately, ROS such as,  $^1\text{O}_2$  also have an obvious inhibitory effect on PGP, so the combination with PDT can significantly improve the efficiency of anti-MDR.

Zeng et al.<sup>[279]</sup> successfully achieved a combined treatment of PDT with chemotherapy by CO assembly of inorganic PSs ( $\text{TiO}_2$ ) and doxorubicin (DOX). The UCNP materials wrapped outside of  $\text{TiO}_2$  can convert the near-infrared into ultra-strong light to excite PS to produce a large amount of ROS, improving the anti-MDR efficiency. The experimental data proved that the combined PDT reduced the viability of target cancer cells by 53.5% and increased the inhibition rate by 90.33% compared with the DOX treatment alone. In a similar study, Chen et al.<sup>[293]</sup> have also successfully developed a nano-drug system that combines DOX-based chemotherapy with PDT. In this system, DOX and Mn ions were co-loaded on the surface of phycocyanin-modified fiber-based nanoparticles. Under the influence of the TME (hypoxia, high concentration of hydrogen peroxide/glutathione), the drug encapsulated by nanoparticles was released efficiently. Dox produces a large amount of Ho during chemotherapy, which is then converted into hydroxyl radical and oxygen by Mn. Under the action of PDT, the generated oxygen generates a high concentration of  $^1\text{O}_2$ , which realizes the cascade reaction. What's more, In order to improve the curative effect, Wang et al. Used chlorine6 (CE6) as PSs and encapsulated with hollow manganese carbonate ( $\text{MnCO}$ ) nanocube to prepare a responsive nano platform for combined therapy.<sup>[294]</sup> The results showed that the combination of chemotherapy and PDT in vivo could remarkably inhibit the growth of tumor, and had no obvious damage to normal tissues.

In addition, the further aggravation of TME hypoxia caused by PDT can enhance the efficacy of some hypoxia-sensitive chemotherapeutic drugs and achieve hypoxia targeting,<sup>[295–299]</sup> as described above in detail.

There is no doubt that the combination of PDT and chemotherapy has a significant synergistic effect, which greatly reduces the side effects of treatment while improving the curative effect. However, the disadvantage of this scheme is that the metabolism speed of PSs and chemotherapeutic drugs in the human body is different. Whether different metabolic rates will interfere with each other and hinder the therapeutic effect needs further research.

### 6.3. Combined Photodynamic Therapy and Immunotherapy

PDT can not only produce an independent killing effect on tumor cells by producing  $^1\text{O}_2$  but also stimulate the human immune system and induce ICD to completely eliminate tumor cells.<sup>[75]</sup> Therefore, PDT can be combined with immunotherapy to play a synergistic effect. On the one hand, PDT can be combined with an immunoadjuvant to enhance the immunogenicity of the tumor. On the other hand, it also can be combined with an immune-checkpoint inhibitor to increase tumor infiltration of cytotoxic  $\text{CD8}^+$  T cells and effector memory T cells. In clinical application, PDT has been combined with immune checkpoint inhibitors to treat refractory head and neck squamous cell carcinoma. Several cases have reported that PDT promotes com-

plete remission, which cannot be achieved by other traditional therapies.<sup>[300]</sup> Although only a few cases have been confirmed clinically, many experimental studies have demonstrated the development potential of this strategy. Kim et al.<sup>[280]</sup> achieved an effective immunotherapy strategy to kill uveal melanoma (UM) through PDT, combined with Rho kinase (ROCK) inhibitor and PD-1/PD-L1 immune checkpoint blocking. This combination therapy can not only target the primary tumor but also treat the metastatic tumor, which brings the dawn for the patients suffering from UM with metastasis rates as high as 50%. The immune response induced by PDT can recruit and activate many kinds of APCs. ROCK inhibitors can induce in situ immunogenicity clearance, and then promote the differentiation of primitive T cells into tumor-specific cytotoxic T cells. In addition, PD-1/PD-L1 immune checkpoint blockade can change the immune phenotype of tumor surface to realize the transition from “cold tumor” to “hot tumor,” which promotes the accumulation of cytotoxic T cells in the tumor site. The experimental results in the mouse model confirmed that the combined effect of PDT and immune drugs could prolong the survival time of the diseased mice compared with the treatment alone. In addition, the inflammatory response induced by PDT also plays an important role in enhancing the immune response. In an innovation strategy, Qi et al.<sup>[301]</sup> made full use of the characteristics that PDT can enhance the infiltration of neutrophils in the tumor site and prepared a nanocomposite named (SA-2@NCs). They used a sialic acid (SA) derivative to coat ibotinib (IBR), to achieve the target of IBR on peripheral blood neutrophils activated by PDT. In the animal experiment of the breast cancer model, the drug delivery efficiency of tumor cells has been significantly improved, which proves the synergistic effect of PDT and chemotherapy.

Although great progress has been made, unfortunately, some limiting factors will still affect the efficacy of combination therapy. For example, disordered blood vessels and high expression of indoleamine 2,3-dioxygenase (IDO) promote the formation of the immunosuppressive TME, which has greatly restricted the therapeutic effect of immunotherapy drugs. In order to overcome this limitation, Zhou et al.<sup>[302]</sup> integrated axinin (AXT) and dextro-1-methyltryptophan (1MT) with chlorin e6 (Ce6), created a new nano platform. AXT is a tyrosine kinase inhibitor, which can improve the distribution of tumor blood vessels; 1MT is an IDO inhibitor, which can reduce the expression of IDO to reduce the immune resistance of the tumor. Based on the reasonable combination of the above drugs, the nano platform successfully solved some limitations of PDT combined with immunotherapy and significantly inhibited tumor growth and metastasis with minimal side effects.

Using PDT to activate the human immune system to produce long-term immunity is one of the most promising methods to achieve the complete elimination of tumor cells. It makes the combined treatment strategy have excellent application prospects. Unfortunately, the antitumor immune response induced by PDT alone is not enough to completely remove residual lesions or metastases. The low effectiveness of memory immunity also limits the long-term therapeutic effect of tumor. Therefore, how to effectively improve tumor immunogenicity and reduce tumor immunosuppression is still a research hotspot.

#### 6.4. Combined Photodynamic Therapy with Other Therapies

With the continuous innovation of cancer treatment, PDT can be combined with more anti-cancer therapies, such as, radiotherapy (RT), gas synergistic therapy, and even Chinese herbal medicine.

The combination of RT and PDT has a synergistic effect. RT can radiate to deep tumors that PDT is not easily accessible, and PDT can, in turn, improve the disadvantage of RT radiation energy dispersion. Liu et al.<sup>[281]</sup> prepared a kind of coordination polymer nanoparticles (CPNs) with both strong RT and PDT effects under X-ray irradiation. In addition, in order to prolong the half-life of CPN in tumor area and increase the drug concentration in tumor cells, they also modified the surface of CPN with dibenzo cyclooctyne. Dibenzo cyclooctyne can be coupled with the azide group on the cell membrane, which is produced by cell glucose metabolism, thus enhancing the biocompatibility of CPN. The experimental results confirmed the high efficiency and low toxicity of CPN. In another study, recently, Zhu et al.<sup>[303]</sup> realized the combination of PDT and NO-based gas therapy. NO can be produced by the oxidation of L-arginine and molecular oxygen by NO synthase. On the one hand, the production of NO affects the energy metabolism of cells, on the other hand, it activates the expression of the p53 tumor suppressor gene to produce an anti-tumor effect. Zhu's team encapsulated arginine and Ce6 (PS) with the same nanoparticles. Under 660 nm laser irradiation, Ce6 produced a large amount of ROS, which not only directly damaged cancer cells but also further oxidized arginine to produce NO, which had a synergistic effect with PDT. As expected, the combination of gas therapy and PDT showed good antitumor activity both in vivo and in vitro. Herbal medicine is a kind of traditional Chinese medicine, some of which can significantly enhance human immunity and produce an anti-tumor effect. These pharmacological values make it possible to combine it with PDT. Astragaloside III (As), as a kind of innate immune activator, has been tried to be combined with PDT. Wu et al.<sup>[304]</sup> constructed a new nanoplatform ([As + Ce6] @ MSNs-PEG) by co entrapping As with Ce6 (PS) with nanoparticles. In experiments using colorectal cancer cells as a model, the nanoplatform successfully activated the maturation of natural killer cells, which in turn promoted the secretion of signaling factors such as interleukins from immune cells and elevated the expression of T-box transcription factors in T cells. The treated mice had an extended lifespan and showed no significant side effects.

Besides, PDT combined with another single therapy still has some limitations in the clinic, so the combination of three or more therapies is gradually becoming a trend. In order to make full use of the advantages of various treatment modes and minimize the dose/PSs and irradiation power/time, many nanoplatforms have been developed for multimodal therapy in recent years.<sup>[305–312]</sup> It provides a broader platform for us to flexibly use PDT in the clinic.

### 7. Recent Advancement in Photodynamic Therapy

Traditional PDT has many limitations, which will not only lead to the unsatisfactory clinical efficacy of PDT but also cause a series of disturbing side effects. Among them, hypoxia is the key limiting factor. On the one hand, it causes dysfunctional neovascularization by affecting the TME and enables tumor de-

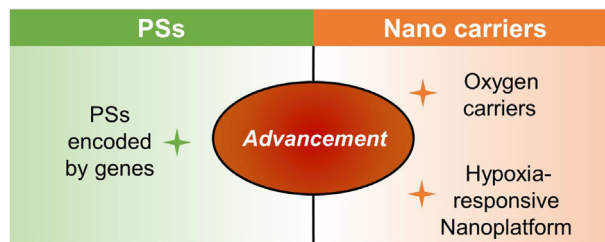


**Figure 12.** Pictorial representation of recent advancements in PDT.

velopment enhancement through cell mobility, invasion, and metastasis.<sup>[313,314]</sup> On the other hand, hypoxia can limit the generation of ROS in the process of PDT, which significantly affects the therapeutic effect. Fortunately, with the rapid development of oxygen carriers, the hypoxia during PDT has been gradually overcome (**Figure 12**). The most commonly used oxygen carrier is hemoglobin (Hb). With the help of ferritin as nano-capsules, Tang et al.<sup>[315]</sup> bound hydrophobic photosensitizer (PSs) (ZnF16Pc) on the surface of RBCs to enhance PDT. However, as an oxygen carrier, Hb has an ideal size, but it also has poor biocompatibility (instability, short half-life).<sup>[316]</sup> In order to solve the above problems, Guo et al.<sup>[317]</sup> combined hemoglobin with ICG to prepare a kind of liposome with biocompatibility. Cell experiments confirmed that the complex significantly enhanced the phototoxicity of tumor cells under hypoxic conditions and improved the efficacy of PDT. Similarly, Luo et al.<sup>[318]</sup> developed a nanohybrid protein oxygen carrier through the disulfide bond recombination of hemoglobin and albumin. The nanocarrier can provide oxygen to improve the production of active oxygen in the PDT process, and successfully break the treatment resistance induced by hypoxia in PDT.

The combination of hypoxia-responsive chemotherapeutic drugs to kill tumor cells under PDT-induced hypoxia has also become one of the development directions of PDT.<sup>[319–321]</sup> Banox-antrone (AQ4N), a hypoxia-activated prodrug that only shows toxicity to cancer cells in a hypoxia environment, has been used to combine with PDT to improve the anti-cancer effect. Feng et al.<sup>[321]</sup> synthesized a multifunctional liposome by combining AQ4N with Ce6 (PS). Compared with the traditional PDT, this new synthetic drug can trigger chemotherapy by using the TME hypoxia induced by PDT, which greatly improves the curative effect. In another study, Zhou et al.<sup>[322]</sup> developed a kind of light-promoted nanoparticles by encapsulating paclitaxel precursor drug with polypeptide copolymer modified by Ce6. PSs Ce6 can not only effectively generate  $^1\text{O}_2$  to kill cancer cells under light, but also promote the release of paclitaxel due to hypoxia. These innovative drug systems show great potential in the treatment of cancer and provide new ideas for the development of PDT in clinical application.

In addition, the improvement of PSs is also in progress. Recently, the development of PSs encoded by genes has become a hot topic. The PSs encoded by gene not only allow PS to express exclusively in tumor cells but also can be manipulated by genetic engineering with a variety of target-specific genes for the precise Spatio-temporal control of ROS generation. Besides, they even endow tumor cells with certain characteristics to make them more suitable for PDT. The red fluorescent protein killer Red is a

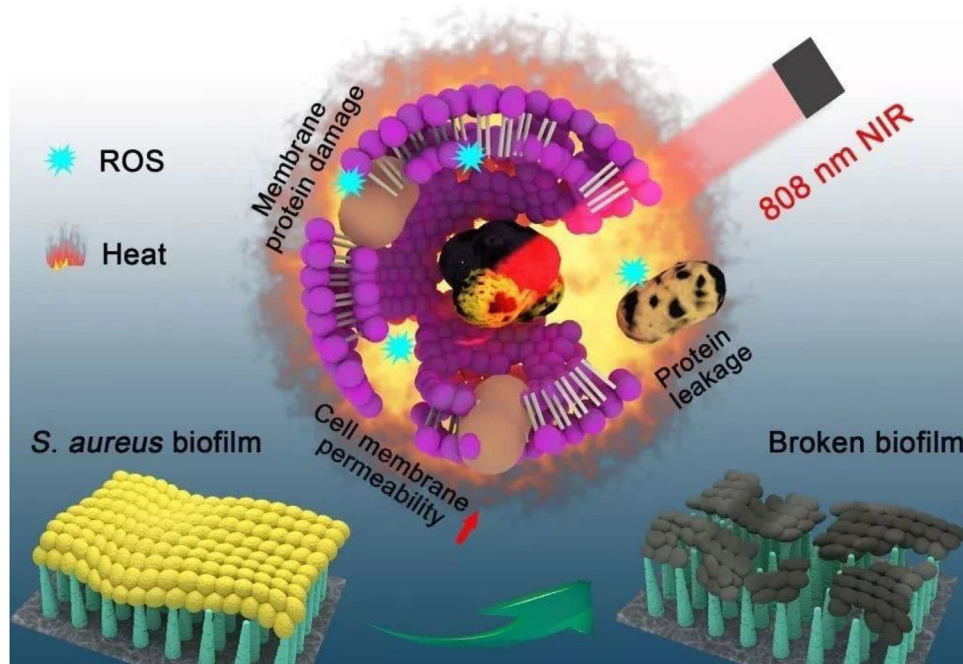


**Figure 13.** Mechanism of PDT to produce an antibacterial effect. Under the irradiation of near-infrared light, PS produces a lot of ROS and heat, which can destroy the bacterial wall/membrane and cause the leakage of the cytoplasm. Reproduced with permission.<sup>[340]</sup> Copyright 2019, WILEY-VCH.

classic gene-encoded PSs. Compared with traditional PSs, killer Red has the advantage that it can precisely damage any desired cell compartment and directly kill cells through expression in tumor cells and appropriate gene transduction.<sup>[323,324]</sup> Recently, Micheletto et al.<sup>[325]</sup> designed a gene coding protein as a PSs. These new PSs can receive the energy transfer of scintillating nanoparticles, which paves the way for the application of PDT in deep tumors.

## 8. Combat Microbial Infection and Resistance

Infection is another very common pathogenic factor besides tumor. Although millions of lives have been successfully saved with the finding of antibodies, however, conventional antibodies presenting some limitations of severe side effects and low utilization rate.<sup>[326–328]</sup> Moreover, in the past decades, miss application and overuse of antibodies also leading to the prevalence of multidrug-resistant (MDR) pathogenic bacteria,<sup>[329,330]</sup> which is becoming a global public health problem. A statistics from World Health Organization (WHO), overuse or misuse of antibiotics has developed nearly 80% of MDR microorganisms. Based on this grim situation, in addition to the development of new antibiotics, put an end to the abuse of antibiotics, it is also necessary to seek innovative antibacterial means. Because of its good controllability and excellent antibacterial ability, PDT has been widely concerned by the medical community.<sup>[331]</sup> It has been reported that ROS produced by PDT, which is mainly  $^1\text{O}_2$ , has a killing effect on both Gram-negative and Gram-positive bacteria<sup>[332,333]</sup> (Figure 13). What is more gratifying is that PDT, as a new non-antibiotic treatment strategy, has an excellent bactericidal effect on the vast majority of MDR bacteria.<sup>[334–336]</sup> Therefore, PDT can not only be used for dental bacteria inactivation,<sup>[337,338]</sup> and

wound healing in dentistry,<sup>[339]</sup> more importantly, it can provide the dawn of cure for patients with MDR bacteria infection.

Zhao et al.<sup>[341]</sup> developed a bacterial-activated photodynamic nano system for PDT-based antimicrobial therapy. They modified Ce6 (PS) in the polyelectrolyte coating on the surface of silica nanoparticles so that the  $^1\text{O}_2$  produced by Ce6 was rapidly quenched and could not exert effective phototoxicity. However, when bacteria extracted polyelectrolyte-ce6 complex from silica nanoparticles, the aggregation state of CE6 was changed, which made CE6 show good phototoxicity again. Subsequently, the  $^1\text{O}_2$  produced by PDT can break the cell wall and cell membrane of bacteria (even MDR bacteria), showing spectral antibacterial activity. Similarly, Lu et al.<sup>[342]</sup> also constructed multifunctional chitosan (CS) encapsulated Ce6 nanoparticles to resist infection caused by multi-drug resistant bacteria (methicillin-resistant *Staphylococcus aureus*). CS has a positive charge on the surface, which can effectively capture bacteria. Combined with PSs Ce6, the nanoparticle shows good photodynamic bactericidal ability in vitro. However, some of the factors, including the high concentrations of glutathione, hypoxic microenvironment at the infection site, the aggregation of the hydrophobic PSs in aqueous media, and the inefficient biodistribution of PS limit its expansion to clinical conditions. In order to overcome these limitations, in addition to the development of a more powerful nano-drug delivery system,<sup>[331]</sup> combination therapy is also an effective solution strategy.

At present, the use of antibiotic-based chemotherapy is the most commonly used method in the clinical treatment of infection. However, due to the limitation of the efficiency of antibiotic administration (oral/intravenous), it generally requires larger dosage to achieve the desired efficacy. This will not only cause unnecessary side effects but also promote the formation

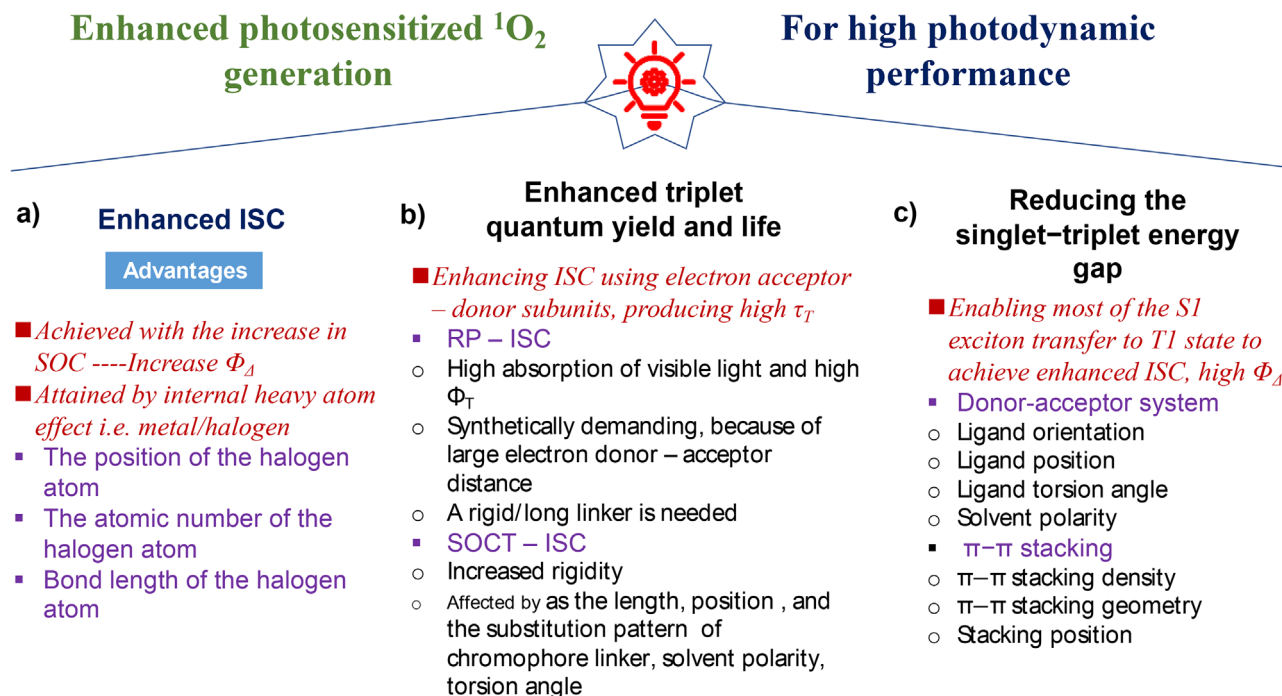


**Figure 14.** Summary of several strategies to improve the  $^1\text{O}_2$  generation and photodynamic performance of PSs.

of drug-resistant bacteria. Therefore, scientists hope that PDT and chemotherapy can learn from each other to form a more efficient antibacterial strategy. Mei et al.<sup>[343]</sup> proposed a highly efficient antibacterial system based on a synergistic combination of PDT/PTT and chemotherapy. This nanosystem is composed of chitosan oligosaccharide coated CE6. Cos has antibacterial activity, while graphene quantum dots can initiate PDT and PTT simultaneously. The synergistic effect of the two makes the cell membrane of bacteria collapse irreversibly, which eventually leads to the death of bacteria.

We consider that the PDT-based nano-system is beneficial in finding applications in environmental science and health that necessitate the monitoring and sterilization of bacteria.

## 9. Summary and Future Perspectives

The demand for the treatment of cancer patients has been vigorously increasing. However, the limitations of conventional treatment modalities have been urging the need for treatment options with suitable options. Recently, PDT demonstrated promising therapeutic efficiency as an alternative to conventional therapeutic modalities due to high selectivity, fewer side effects, efficient cosmetic outcomes, and safe repeatability. Moreover, with the development of nanotechnology, the previous limitations of PDT have been effectively solved, which makes the applicable types of cancer have been significantly increased. PDT works on a simple mechanism, but several parameters have been involved in which is making it a complicated process, and more in-depth study is needed to determine parameters of optimized performance. In recent years, several reports have been published describing the overwhelming advantages of  $^1\text{O}_2$  over other ROS including high reactivity, oxidative ability, moderate energy gap, and potential to

be free from other contaminants. In addition to the above advantages,  $^1\text{O}_2$  can also react with a variety of cellular components, resulting in significant cytotoxic effects. After damaging a variety of important macromolecules in cancer cells,  $^1\text{O}_2$  will activate a series of cell signaling pathways and induce cancer cell apoptosis. These multiple mechanisms ensure the killing ability of PDT to tumors.

Regarding enhancement in  $^1\text{O}_2$  generation, the modification methods have been classified into three main categories (ISC, triplet quantum yield and life, and singlet-triplet energy gap) based on their photophysical properties of PSs. First, the enhancement in the singlet-triplet ISC rates has been attained by improving the SOC with the introduction of heavy atoms (i.e., metal or halogens) that are beneficial in achieving enhanced  $\Phi_{\Delta}$  (Figure 14a). The position of the halogen atom into the PSs, bond length, and an atomic number of halogen also affect the enhancement in  $\Phi_{\Delta}$ . The ISC transition time decreases sharply with the increase in atomic weight of halogen, decrease in bond length, and the number of halogen atoms. However, the introduction of a heavy atom induces several limitations such as, high cost, tedious synthesis, the low solubility of PSs, and dark toxicity. In this regard, photoinduced electron transfer is an attractive approach of improving ISC using electron acceptor–donor subunits, producing high  $\tau_T$  (Figure 14b). The position, length, and pattern of electron acceptor–donor chromophore determine the fate of ISC. Generally, the small chromophore linker length presents high  $\Phi_T$  and decreases with the retardation of angle. Third, a decrease in  $\Delta E_{ST}$  by electron donor-acceptor system and  $\pi$ – $\pi$  stacking is also advantageous in enhanced  $^1\text{O}_2$  generation by improving the TSP (Figure 14c).

Generally,  $^1\text{O}_2$  showed a small lifetime thus their reactivity is limited to nearby biological molecules which are requiring

localized delivery of PSs. In this situation, nanocarriers emerge as the times require, and bring PDT to a new height. Nanocarriers can achieve high concentration aggregation of PSS inside tumor cells and reduce the phototoxicity of PDT to human normal tissues. In addition, the nanocarrier can also make the PSS locate with specific organelles, which maximizes the cytotoxicity of  $^1\text{O}_2$ . Furthermore, some nanocarriers (liposomes, etc.) can increase the accumulation rate of PSS in tumors and improve the biocompatibility of drugs. It makes the side effects of the whole drug delivery system greatly reduced and lays a solid foundation for the clinical application of PDT.

After the destruction of important organelles in tumor cells by  $^1\text{O}_2$ , the body's immune system will be activated immediately. Through active immunity and adaptive immunity, the residual tumor cells can be removed spontaneously. In addition to killing tumor cells independently, PDT combined with other traditional treatment strategies also shows great potential in cancer treatment. On the one hand, the unique cytotoxicity of PDT, which depends on  $^1\text{O}_2$ , can help the traditional treatment to reduce the drug resistance and the occurrence of tumor escape. On the other hand, PDT has the characteristics of low invasiveness and few side effects, which makes it a perfect choice for combination therapy. The solution of hypoxia and the emergence of gene encoding PS further improve the practicability of PDT in clinical cancer treatment. In addition, the good bactericidal ability of  $^1\text{O}_2$  allows PDT to become a new anti-infection strategy. At the moment of bacteria mutation, antibiotic therapy alone has been unable to meet the infection caused by some "super bacteria." And PDT may become a new weapon for the treatment of these MDR bacterial infections.

With the intensive study on this research field, exhilarating progress has been done in the past decade. However, several challenges persist and entail further study, which also provides chances for future research.

The  $^1\text{O}_2$  generation is much slower in most of the published reports due to slow ISC rates. Future work may focus on the conjugation of donor–acceptor–donor triad to tune the photophysical properties of the backbone to tune the SOCT-ICT mechanism by developing donor— $\pi$ -bridge-acceptor— $\pi$ -bridge-donor system.<sup>[180]</sup> To further improve the  $^1\text{O}_2$  generation and localized delivery of PSs, future work may focus on further modification in nanocarrier systems. Specifically, for fiber optic technology, some revolutionary research has shown that a high dosage of light delivery can be achieved along with decreased photocytotoxicity in the non-targeted region.<sup>[262]</sup> Such an interesting area of research needs further investigation for improving light and PSs delivery to guarantee large production of  $^1\text{O}_2$ .

To further enhance the therapeutic effect of  $^1\text{O}_2$ , inducing ICD of tumor cells and combining with multiple treatment modes are effective methods. Among them, inducing ICD may cure the tumor completely. Therefore, how to prevent tumor immune escape and how to successfully induce ICD to become the top priority. It is known that the damage of the endoplasmic reticulum can cause ICD,<sup>[271]</sup> so how to make  $^1\text{O}_2$  effectively accumulate in the endoplasmic reticulum may become one of the research goals. In addition, immune adjuvants and immune checkpoint inhibitors can increase the immunogenicity of tumor cells and improve the success rate of ICD induction. The current clinical data show that only a few cases can get significant remission when PDT is com-

bined with the above drugs. In this case, how to improve PS or drug delivery system to better combine with immunotherapy remains to be explored. The combination of PDT and multiple therapeutic strategies to form triple therapy or more is also considered to have great prospects. However, it is a great challenge to concentrate so many reactions into one drug, which puts forward higher requirements for PSs and nano-drug delivery platforms.

## Acknowledgements

Z.Y.J. and H.F. contributed equally to this work. This work was supported by the Australian Research Council Discovery Project, Grant No. DP200103332 and DP200103315.

## Conflict of interest

The authors declare no conflict of interest.

## Keywords

intersystem crossing, photodynamic therapy, singlet oxygen, singlet-triplet energy gap, triplet quantum yield, Triplet quantum life

Received: August 15, 2021

Revised: October 5, 2021

Published online: November 12, 2021

- [1] R. R. Allison, K. Moghissi, *Clin. Endosc.* **2013**, 46, 24.
- [2] H. Abrahamse, M. R. Hamblin, *Biochem. J.* **2016**, 473, 347.
- [3] P. Zhang, H. Huang, S. Banerjee, G. J. Clarkson, C. Ge, C. Imberti, P. J. Sadler, *Angew. Chem., Int. Ed. Engl.* **2019**, 58, 2350.
- [4] M. R. Azhar, Y. Arafat, M. Khiadani, S. Wang, Z. Shao, *Composites, Part B* **2020**, 192, 107985.
- [5] J. Tian, W. Zhang, *Prog. Polym. Sci.* **2019**, 95, 65.
- [6] X. Feng, H. Guo, K. Patel, H. Zhou, X. Lou, *Chem. Eng. J.* **2014**, 244, 327.
- [7] A. K. Bhatta, P. Wang, U. Keyal, Z. Zhao, J. Ji, L. Zhu, X. Wang, G. Zhang, *Photodiagn. Photodyn. Ther.* **2018**, 23, 273.
- [8] A. E. O'Connor, W. M. Gallagher, A. T. Byrne, *Photochem. Photobiol.* **2009**, 85, 1053.
- [9] R. R. Allison, K. Moghissi, *Clin. Endosc.* **2013**, 46, 24.
- [10] P. Agostinis, K. Berg, K. A. Cengel, T. H. Foster, A. W. Girotti, S. O. Gollnick, S. M. Hahn, M. R. Hamblin, A. Juzeniene, D. Kessel, *Ca-Cancer J. Clin.* **2011**, 61, 250.
- [11] S. B. Brown, E. A. Brown, I. Walker, *Lancet Oncol.* **2004**, 5, 497.
- [12] R. L. Yanovsky, D. W. Bartenstein, G. S. Rogers, S. J. Isakoff, S. T. Chen, *Photodermatol., Photoimmunol. Photomed.* **2019**, 35, 295.
- [13] C. Haak, K. Togsverd-Bo, D. Thaysen-Petersen, H. Wulf, U. Paasch, R. Anderson, M. Haedersdal, *Br. J. Dermatol.* **2015**, 172, 215.
- [14] E. J. Hong, D. G. Choi, M. S. Shim, *Acta Pharm. Sin. B* **2016**, 6, 297.
- [15] J. Zhang, C. Jiang, J. F. Longo, R. Azevedo, H. Zhang, L. Muehlmann, *Acta Pharm. Sin. B* **2018**, 8, 137.
- [16] S. Qi, L. Guo, S. Yan, R. Lee, S. Yu, S. Chen, *Acta Pharm. Sin. B* **2019**, 9, 279.
- [17] P. Agostinis, K. Berg, K. Cengel, T. Foster, A. Girotti, S. Gollnick, S. Hahn, M. Hamblin, A. Juzeniene, D. Kessel, M. Korbelik, J. Moan, P. Mroz, D. Nowis, J. Piette, B. Wilson, J. Golab, *Ca-Cancer J. Clin.* **2011**, 61, 250.
- [18] C. Xu, J. Nam, H. Hong, Y. Xu, J. Moon, *ACS Nano* **2019**, 13, 12148.

- [19] R. Bissonnette, J. Tremblay, P. Juzenas, M. Boushira, H. Lui, *J. Invest. Dermatol.* **2002**, *119*, 77.
- [20] E. Ross, R. Romero, N. Kollias, C. Crum, R. Anderson, *Br. J. Dermatol.* **1997**, *137*, 736.
- [21] B. Giomi, F. Pagnini, A. Cappuccini, B. Bianchi, L. Tiradritti, G. Zucati, *Br. J. Dermatol.* **2011**, *164*, 448.
- [22] C. Morton, L. Braathen, *Am. J. Clin. Dermatol.* **2018**, *19*, 647.
- [23] A. Dijkstra, I. Majoie, J. van Dongen, H. van Weelden, W. van Vloten, *J. Eur. Acad. Dermatol. Venereol.* **2001**, *15*, 550.
- [24] S. Fijan, H. Hönigsmann, B. Ortel, *Br. J. Dermatol.* **1995**, *133*, 282.
- [25] K. Svanberg, T. Andersson, D. Killander, I. Wang, U. Stenram, S. Andersson-Engels, R. Berg, J. Johansson, S. Svanberg, *Br. J. Dermatol.* **1994**, *130*, 743.
- [26] E. de Haas, H. de Vijlder, H. Sterenborg, H. Neumann, D. Robinson, *J. Eur. Acad. Dermatol. Venereol.* **2008**, *22*, 426.
- [27] E. de Haas, B. Kruijt, H. Sterenborg, H. M. Neumann, D. Robinson, *J. Invest. Dermatol.* **2006**, *126*, 2679.
- [28] A. Master, M. Livingston, A. S. Gupta, *J. Controlled Release* **2013**, *168*, 88.
- [29] Y. Yang, Y. Li, L. Zhu, H. He, L. Hu, J. Huang, F. Hu, B. He, Z. Ye, *Nanoscale* **2013**, *5*, 10461.
- [30] L. Benov, *Med. Princ. Pract.* **2015**, *24*, 14.
- [31] J. Shen, T. W. Rees, L. Ji, H. Chao, *Coord. Chem. Rev.* **2021**, *443*, 214016.
- [32] S. Liu, G. Feng, B. Z. Tang, B. Liu, *Chem. Sci.* **2021**, *12*, 6488.
- [33] Y. Liu, R. Qin, S. A. Zaat, E. Breukink, M. Heger, *J. Clin. Transl. Res.* **2015**, *1*, 140.
- [34] L. Huang, S. Zhao, J. Wu, L. Yu, N. Singh, K. Yang, M. Lan, P. Wang, J. S. Kim, *Coord. Chem. Rev.* **2021**, *438*, 213888.
- [35] F. Wei, T. W. Rees, X. Liao, L. Ji, H. Chao, *Coord. Chem. Rev.* **2020**, *432*, 213714.
- [36] W. Tang, Z. Zhen, M. Wang, H. Wang, Y. J. Chuang, W. Zhang, G. D. Wang, T. Todd, T. Cowger, H. Chen, *Adv. Funct. Mater.* **2016**, *26*, 1757.
- [37] H. Wang, X. Yang, W. Shao, S. Chen, J. Xie, X. Zhang, J. Wang, Y. Xie, *J. Am. Chem. Soc.* **2015**, *137*, 11376.
- [38] J. Tian, B. Huang, M. H. Nawaz, W. Zhang, *Coord. Chem. Rev.* **2020**, *420*, 213410.
- [39] A. Jańczyk, E. Krakowska, G. Stochel, W. Macyk, *J. Am. Chem. Soc.* **2006**, *128*, 15574.
- [40] Z. Liu, T. Cao, Y. Xue, M. Li, M. Wu, J. W. Engle, Q. He, W. Cai, M. Lan, W. Zhang, *Angew. Chem.* **2020**, *132*, 3740.
- [41] G. Pasparakis, *Small* **2013**, *9*, 4130.
- [42] L. Misba, S. Zaidi, A. Khan, *J. Photochem. Photobiol., B* **2018**, *183*, 16.
- [43] D. Min, J. Boff, *Compr. Rev. Food Sci. Food Saf.* **2002**, *1*, 58.
- [44] T. Devasagayam, J. P. Kamat, *Indian J. Exp. Biol.* **2002**, *40*, 680.
- [45] A. Castano, T. Demidova, M. Hamblin, *Photodiagn. Photodyn. Ther.* **2004**, *1*, 279.
- [46] S. Li, X. Shen, Q.-H. Xu, Y. Cao, *Nanoscale* **2019**, *11*, 19551.
- [47] M. S. Baptista, J. Cadet, P. Di Mascio, A. A. Ghogare, A. Greer, M. R. Hamblin, C. Lorente, S. C. Nunez, M. S. Ribeiro, A. H. Thomas, *Photochem. Photobiol.* **2017**, *93*, 912.
- [48] H. Abrahamse, C. A. Kruger, S. Kadanyo, A. Mishra, *Photomed. Laser Surg.* **2017**, *35*, 581.
- [49] M. C. DeRosa, R. J. Crutchley, *Coord. Chem. Rev.* **2002**, *233*, 351.
- [50] J. J. Nogueira, M. Oppel, L. González, *Angew. Chem., Int. Ed.* **2015**, *54*, 4375.
- [51] T. J. Penfold, E. Gindensperger, C. Daniel, C. M. Marian, *Chem. Rev.* **2018**, *118*, 6975.
- [52] S. Fukuzumi, K. Ohkubo, T. Suenobu, *Acc. Chem. Res.* **2014**, *47*, 1455.
- [53] Z. Wang, L. Huang, Y. Yan, A. M. El-Zohry, A. Toffoletti, J. Zhao, A. Barbon, B. Dick, O. F. Mohammed, G. Han, *Angew. Chem.* **2020**, *132*, 16248.
- [54] H. Qiu, M. Tan, T. Y. Ohulchanskyy, J. F. Lovell, G. Chen, *Nanomater* **2018**, *8*, 344.
- [55] J. Jiang, Y. Qian, Z. Xu, Z. Lv, P. Tao, M. Xie, S. Liu, W. Huang, Q. Zhao, *Chem. Sci.* **2019**, *10*, 5085.
- [56] V.-N. Nguyen, A. Kumar, M. H. Lee, J. Yoon, *Coord. Chem. Rev.* **2020**, *425*, 213545.
- [57] G. M. F. Calixto, J. Bernegossi, L. M. De Freitas, C. R. Fontana, M. Chorilli, *Molecules* **2016**, *21*, 342.
- [58] D. Van Straten, V. Mashayekhi, H. S. De Bruijn, S. Oliveira, D. J. Robinson, *Cancers* **2017**, *9*, 19.
- [59] S. H. Voon, L. V. Kiew, H. B. Lee, S. H. Lim, M. I. Noordin, A. Kamkaew, K. Burgess, L. Y. Chung, *Small* **2014**, *10*, 4993.
- [60] D. Hu, L. Chen, Y. Qu, J. Peng, B. Chu, K. Shi, Y. Hao, L. Zhong, M. Wang, Z. Qian, *Theranostics* **2018**, *8*, 1558.
- [61] A. Siriviriyannun, Y.-J. Tsai, S. H. Voon, S. F. Kiew, T. Imae, L. V. Kiew, C. Y. Looi, W. F. Wong, H. B. Lee, L. Y. Chung, *Mater. Sci. Eng., C* **2018**, *89*, 307.
- [62] B. J. Quirk, G. Brandal, S. Donlon, J. C. Vera, T. S. Mang, A. B. Foy, S. M. Lew, A. W. Girotti, S. Jugal, P. S. LaViolette, *Photodiagn. Photodyn. Ther.* **2015**, *12*, 530.
- [63] Y.-W. An, H.-T. Jin, B. Yuan, J.-C. Wang, C. Wang, H.-Q. Liu, *Oncol. Lett.* **2021**, *21*, 1.
- [64] G. Xiao, T. Xu, M. Faheem, Y. Xi, T. Zhou, H. T. Moryani, J. Bao, J. Du, *Int. J. Environ. Res. Public Health* **2021**, *18*, 3344.
- [65] C. Huang, C. Zhang, D. Huang, D. Wang, S. Tian, R. Wang, Y. Yang, W. Wang, F. Qin, *Chem. Eng. J.* **2020**, *404*, 127066.
- [66] I. Pibiri, S. Buscemi, A. P. Piccionello, A. Pace, *ChemPhotoChem* **2018**, *2*, 535.
- [67] J. Hynek, M. K. Chahal, D. T. Payne, J. Labuta, J. P. Hill, *Coord. Chem. Rev.* **2020**, *425*, 213541.
- [68] W. Yu, L. Zhao, *TrAC, Trends Anal. Chem.* **2021**, *136*, 116197.
- [69] M. Hardy, J. Zielonka, H. Karoui, A. Sikora, R. Michalski, R. Podsiadly, M. Lopez, J. Vasquez-Vivar, B. Kalyanaraman, O. Ouari, *Antioxid. Redox Signaling* **2018**, *28*, 1416.
- [70] M. Khuli, N. Fazouan, H. A. El Makarim, G. El Halani, E. H. Atmani, *J. Alloys Compd.* **2016**, *688*, 368.
- [71] J. Woolley, J. Stanicka, T. Cotter, *Trends Biochem. Sci.* **2013**, *38*, 556.
- [72] Y. You, *Org. Biomol. Chem.* **2018**, *16*, 4044.
- [73] P. Di Mascio, G. Martinez, S. Miyamoto, G. Ronsein, M. Medeiros, J. Cadet, *Chem. Rev.* **2019**, *119*, 2043.
- [74] A. Girotti, *J. Photochem. Photobiol., B* **2001**, *63*, 103.
- [75] A. Castano, P. Mroz, M. Hamblin, *Nat. Rev. Cancer* **2006**, *6*, 535.
- [76] A. Girotti, *J. Lipid Res.* **1998**, *39*, 1529.
- [77] T. Genaro-Mattos, R. Queiroz, D. Cunha, P. Appolinario, P. Di Mascio, I. Nantes, O. Augusto, S. Miyamoto, *Biochemistry* **2015**, *54*, 2841.
- [78] J. Angeli, C. Garcia, F. Sena, F. Freitas, S. Miyamoto, M. Medeiros, P. Di Mascio, *Free Radical Biol. Med.* **2011**, *51*, 503.
- [79] S. Dixon, K. Lemberg, M. Lamprecht, R. Skouta, E. Zaitsev, C. Gleason, D. Patel, A. Bauer, A. Cantley, W. Yang, B. Morrison, B. Stockwell, *Cell* **2012**, *149*, 1060.
- [80] W. Nes, *Chem. Rev.* **2011**, *111*, 6423.
- [81] A. Vila, W. Korytowski, A. Girotti, *Biochemistry* **2002**, *41*, 13705.
- [82] J. Stone, S. Yang, *Antioxid. Redox Signaling* **2006**, *8*, 243.
- [83] J. Cadet, K. Davies, M. Medeiros, P. Di Mascio, J. Wagner, *Free Radical Biol. Med.* **2017**, *107*, 13.
- [84] J. Cadet, J. Ravanat, M. TavernaPorro, H. Menoni, D. Angelov, *Cancer Lett.* **2012**, *327*, 5.
- [85] J. Cadet, T. Douki, J. Ravanat, *Mutat. Res.* **2011**, *711*, 3.
- [86] P. Dedon, *Chem. Res. Toxicol.* **2008**, *21*, 206.
- [87] J. Cadet, T. Douki, J. Ravanat, *Acc. Chem. Res.* **2008**, *41*, 1075.

- [88] J. Cadet, T. Douki, J. Ravanat, *Photochem. Photobiol.* **2015**, *91*, 140.
- [89] A. Jiménez-Banzo, M. Sagristà, M. Mora, S. Nonell, *Free Radical Biol. Med.* **2008**, *44*, 1926.
- [90] M. Westberg, M. Bregnhøj, C. Banerjee, A. Blázquez-Castro, T. Breitenbach, P. Ogilby, *Methods* **2016**, *109*, 81.
- [91] M. Simon, H. Van Vunakis, *J. Mol. Biol.* **1962**, *4*, 488.
- [92] E. Dumont, R. Grüber, E. Bignon, C. Morell, J. Aranda, J. Ravanat, I. Tuñón, *Chem* **2016**, *22*, 12358.
- [93] E. Dumont, R. Grüber, E. Bignon, C. Morell, Y. Moreau, A. Monari, J. Ravanat, *Nucleic Acids Res.* **2016**, *44*, 56.
- [94] W. Wang, M. Zhao, Y. Zhao, W. Shen, S. Yin, *Environ. Pollut.* **2020**, *263*, 114534.
- [95] S. Orrenius, V. Gogvadze, B. Zhivotovsky, *Annu. Rev. Pharmacol. Toxicol.* **2007**, *47*, 143.
- [96] S. Zhuang, J. Demirs, I. Kochevar, *J. Biol. Chem.* **2000**, *275*, 25939.
- [97] W. Chan, J. Yu, S. Yang, *Biochem. J.* **2000**, *351*, 221.
- [98] A. Agarwal, S. Gupta, R. K. Sharma, *Reprod. Biol. Endocrinol.* **2005**, *3*, 28.
- [99] D. Fruman, C. Rommel, *Nat. Rev. Drug Discovery* **2014**, *13*, 140.
- [100] A. R. Amin, T. Senga, M. Oo, A. Thant, M. Hamaguchi, *Genes Cells* **2003**, *8*, 515.
- [101] L. Chang, P. Graham, J. Hao, J. Ni, J. Bucci, P. Cozzi, J. Kearsley, Y. Li, *Cell Death Dis.* **2013**, *4*, e875.
- [102] S. Kang, T. Kwon, D. Kwon, S. Do, *J. Biol. Chem.* **1999**, *274*, 13085.
- [103] N. Leslie, *Antioxid. Redox Signaling* **2006**, *8*, 1765.
- [104] I. Engelmänn, S. Dormann, M. Saran, G. Bauer, *Redox Rep.* **2000**, *5*, 207.
- [105] M. Herdener, S. Heigold, M. Saran, G. Bauer, *Free Radical Biol. Med.* **2000**, *29*, 1260.
- [106] G. Bauer, *Anticancer Res.* **2012**, *32*, 2599.
- [107] G. Bauer, *Anticancer Res.* **2014**, *34*, 1467.
- [108] J. Escobar, M. Rubio, E. Lissi, *Free Radical Biol. Med.* **1996**, *20*, 285.
- [109] K. Scheit, G. Bauer, *Carcinogen* **2015**, *36*, 400.
- [110] E. Goldman, L. Chen, H. Fu, *J. Biol. Chem.* **2004**, *279*, 10442.
- [111] H. Ichijo, E. Nishida, K. Irie, P. ten Dijke, M. Saitoh, T. Moriguchi, M. Takagi, K. Matsumoto, K. Miyazono, Y. Gotoh, *Science* **1997**, *275*, 90.
- [112] K. Tobiume, A. Matsuzawa, T. Takahashi, H. Nishitoh, K. Morita, K. Takeda, O. Minowa, K. Miyazono, T. Noda, H. Ichijo, *EMBO Rep.* **2001**, *2*, 222.
- [113] D. Dhanasekaran, E. Reddy, *Oncogene* **2008**, *27*, 6245.
- [114] F. Hu, S. Xu, B. Liu, *Adv. Mater.* **2018**, *30*, 1801350.
- [115] J. Al Anshori, T. Slanina, E. Palao, P. Klán, *Photochem. Photobiol. Sci.* **2016**, *15*, 250.
- [116] A. Rodriguez-Serrano, V. Rai-Constapel, M. C. Daza, M. Doerr, C. M. Marian, *Phys. Chem. Chem. Phys.* **2015**, *17*, 11350.
- [117] L. Zhou, S. Wei, X. Ge, J. Zhou, B. Yu, J. Shen, *J. Phys. Chem. B* **2012**, *116*, 12744.
- [118] M. Kasha, *J. Chem. Phys.* **1952**, *20*, 71.
- [119] A. Kearvell, F. Wilkinson, *Mol. Cryst.* **1968**, *4*, 69.
- [120] T. Y. Ohulchanskyy, D. J. Donnelly, M. R. Detty, P. N. Prasad, *J. Phys. Chem. B* **2004**, *108*, 8668.
- [121] S. Hirohara, Y. Kawasaki, R. Funasako, N. Yasui, M. Totani, H. Alitomo, J. Yuasa, T. Kawai, C. Oka, M. Kawaichi, *Bioconjugate Chem.* **2012**, *23*, 1881.
- [122] L. Zhou, X. Ge, J. Liu, J. Zhou, S. Wei, F. Li, J. Shen, *Bioorg. Med. Chem. Lett.* **2013**, *23*, 5317.
- [123] Z. He, W. Zhao, J. W. Lam, Q. Peng, H. Ma, G. Liang, Z. Shuai, B. Z. Tang, *Nat. Commun.* **2017**, *8*, 416.
- [124] Y. Lee, R. M. Malamakal, D. M. Chenoweth, J. M. Anna, *J. Phys. Chem. Lett.* **2020**, *11*, 877.
- [125] M. Einzinger, T. Zhu, P. de Silva, C. Belger, T. M. Swager, T. Van Voorhis, M. A. Baldo, *Adv. Mater.* **2017**, *29*, 1701987.
- [126] W. Hu, T. He, H. Zhao, H. Tao, R. Chen, L. Jin, J. Li, Q. Fan, W. Huang, A. Baev, *Angew. Chem., Int. Ed.* **2019**, *58*, 11105.
- [127] B. C. De Simone, G. Mazzone, N. Russo, E. Sicilia, M. Toscano, *Phys. Chem. Chem. Phys.* **2018**, *20*, 2656.
- [128] D. S. McClure, *J. Chem. Phys.* **1949**, *17*, 665.
- [129] J. Zou, Z. Yin, K. Ding, Q. Tang, J. Li, W. Si, J. Shao, Q. Zhang, W. Huang, X. Dong, *ACS Appl. Mater. Interfaces* **2017**, *9*, 32475.
- [130] K. Hayashi, M. Nakamura, H. Miki, S. Ozaki, M. Abe, T. Matsumoto, T. Kori, K. Ishimura, *Adv. Funct. Mater.* **2014**, *24*, 503.
- [131] A. D. Quartarolo, S. G. Chiodo, N. Russo, *J. Chem. Theory Comput.* **2010**, *6*, 3176.
- [132] A. Kamkaew, S. H. Lim, H. B. Lee, L. V. Kiew, L. Y. Chung, K. Burgess, *Chem. Soc. Rev.* **2013**, *42*, 77.
- [133] S. Guo, L. Ma, J. Zhao, B. Küçüköz, A. Karatay, M. Hayvali, H. G. Yaglioglu, A. Elmali, *Chem. Sci.* **2014**, *5*, 489.
- [134] S. J. Ang, T. S. Chwee, M. W. Wong, *J. Phys. Chem. C* **2018**, *122*, 12441.
- [135] B. C. De Simone, G. Mazzone, J. Pirillo, N. Russo, E. Sicilia, *Phys. Chem. Chem. Phys.* **2017**, *19*, 2530.
- [136] B. Kim, B. Sui, X. Yue, S. Tang, M. G. Tichy, K. D. Belfield, *Eur. J. Org. Chem.* **2017**, *2017*, 25.
- [137] A. Gorman, J. Killoran, C. O'Shea, T. Kenna, W. M. Gallagher, D. F. O'Shea, *J. Am. Chem. Soc.* **2004**, *126*, 10619.
- [138] V. P. Torchilin, *Pharm. Res.* **2007**, *24*, 1.
- [139] A. Serra, M. Pineiro, C. I. Santos, A. M. d. A. R. Gonsalves, M. Abrantes, M. Laranjo, M. F. Botelho, *Photochem. Photobiol.* **2010**, *86*, 206.
- [140] S. Kim, T. Y. Ohulchanskyy, D. Bharali, Y. Chen, R. K. Pandey, P. N. Prasad, *J. Phys. Chem. C* **2009**, *113*, 12641.
- [141] Y. Zhang, Z. Yang, X. Zheng, L. Yang, N. Song, L. Zhang, L. Chen, Z. Xie, *Dyes Pigm.* **2020**, *178*, 108348.
- [142] W. Zhou, Y. Chen, Y. Zhang, X. Xin, R. Li, C. Xie, Q. Fan, *Small* **2020**, *16*, 1905641.
- [143] L.-L. Zhou, Q. Guan, Y.-A. Li, Y. Zhou, Y.-B. Xin, Y.-B. Dong, *Inorg. Chem.* **2018**, *57*, 3169.
- [144] J. Zhao, K. Chen, Y. Hou, Y. Che, L. Liu, D. Jia, *Org. Biomol. Chem.* **2018**, *16*, 3692.
- [145] M. Hussain, J. Zhao, W. Yang, F. Zhong, A. Karatay, H. G. Yaglioglu, E. A. Yildiz, M. Hayvali, *J. Lumin.* **2017**, *192*, 211.
- [146] V.-N. Nguyen, S. Qi, S. Kim, N. Kwon, G. Kim, Y. Yim, S. Park, J. Yoon, *J. Am. Chem. Soc.* **2019**, *141*, 16243.
- [147] J. Xu, H. Liu, Y. S. Meng, *Electrochem. Commun.* **2015**, *60*, 13.
- [148] G. Bottari, G. de la Torre, D. M. Guldi, T. Torres, *Chem. Rev.* **2010**, *110*, 6768.
- [149] M. A. Filatov, S. Karuthedath, P. M. Polestshuk, S. Callaghan, K. J. Flanagan, T. Wiesner, F. Laquai, M. O. Senge, *ChemPhotoChem* **2018**.
- [150] J. M. Lee, S. Kang, T. G. Hwang, H. M. Kim, W. S. Lee, D. Kim, J. P. Kim, *Dyes Pigm.* **2021**, *187*, 109051.
- [151] A. Mukhopadhyay, V. K. Maka, J. N. Moorthy, *Phys. Chem. Chem. Phys.* **2017**, *19*, 4758.
- [152] M. A. Collini, M. B. Thomas, V. Bandi, P. A. Karr, F. D'Souza, *Chem. - Eur. J.* **2017**, *23*, 4450.
- [153] X. F. Zhang, N. Feng, *Chem. - Asian J.* **2017**, *12*, 2447.
- [154] M. A. Filatov, *Org. Biomol. Chem.* **2020**, *18*, 10.
- [155] Z. Wang, Y. Gao, M. Hussain, S. Kundu, V. Rane, M. Hayvali, E. A. Yildiz, J. Zhao, H. G. Yaglioglu, R. Das, *Chem. - Eur. J.* **2018**, *24*, 18663.
- [156] Y. Hou, I. Kurganskii, A. Elmali, H. Zhang, Y. Gao, L. Lv, J. Zhao, A. Karatay, L. Luo, M. Fedin, *J. Chem. Phys.* **2020**, *152*, 114701.
- [157] M. T. Colvin, A. B. Ricks, A. M. Scott, D. T. Co, M. R. Wasielewski, *J. Phys. Chem. A* **2012**, *116*, 1923.
- [158] Z. Wang, J. Zhao, *Org. Lett.* **2017**, *19*, 4492.
- [159] L. Kong, Z. Huang, P. Chen, H. Wang, S. Zhu, J. Yang, *Dyes Pigm.* **2020**, *173*, 107886.



- [160] Z. E. Dance, S. M. Mickley, T. M. Wilson, A. B. Ricks, A. M. Scott, M. A. Ratner, M. R. Wasielewski, *J. Phys. Chem. A* **2008**, *112*, 4194.
- [161] Y. Hou, T. Biskup, S. Rein, Z. Wang, L. Bussotti, N. Russo, P. Foggi, J. Zhao, M. Di Donato, G. Mazzone, *J. Phys. Chem. C* **2018**, *122*, 27850.
- [162] Z. Li, B. Li, X. Wei, J. Liu, R. Wang, X. Hu, G. Liu, H. Gao, Y. Zhang, C.-S. Lee, *Appl. Phys. Lett.* **2019**, *115*, 263302.
- [163] N. Rehmat, A. Toffoletti, Z. Mahmood, X. Zhang, J. Zhao, A. Barbon, *J. Mater. Chem. C* **2020**, *8*, 4701.
- [164] Y. Hou, Q. Liu, J. Zhao, *Chem. Commun.* **2020**, *56*, 1721.
- [165] M. A. Filatov, S. Karuthedath, P. M. Polestshuk, H. Savoie, K. J. Flanagan, C. Sy, E. Sitte, M. Telitchko, F. Laquai, R. W. Boyle, *J. Am. Chem. Soc.* **2017**, *139*, 6282.
- [166] Z. Wang, M. Ivanov, Y. Gao, L. Bussotti, P. Foggi, H. Zhang, N. Russo, B. Dick, J. Zhao, M. Di Donato, *Chem. - Eur. J.* **2020**, *26*, 1091.
- [167] H. Liang, S. Sun, M. Zafar, Z. Yuan, Y. Dong, S. Ji, Y. Huo, J. Zhao, *Dyes Pigm.* **2020**, *173*, 108003.
- [168] L. Huang, J. Zhao, S. Guo, C. Zhang, J. Ma, *J. Org. Chem.* **2013**, *78*, 5627.
- [169] K. Chen, W. Yang, Z. Wang, A. Iagatti, L. Bussotti, P. Foggi, W. Ji, J. Zhao, M. Di Donato, *J. Phys. Chem. A* **2017**, *121*, 7550.
- [170] M. Imran, A. A. Sukhanov, Z. Wang, A. Karatay, J. Zhao, Z. Mahmood, A. Elmali, V. K. Voronkova, M. Hayvali, Y. H. Xing, *J. Phys. Chem. C* **2019**, *123*, 7010.
- [171] M. A. Filatov, S. Karuthedath, P. M. Polestshuk, S. Callaghan, K. J. Flanagan, M. Telitchko, T. Wiesner, F. Laquai, M. O. Senge, *Phys. Chem. Chem. Phys.* **2018**, *20*, 8016.
- [172] Y. Zhao, A. A. Sukhanov, R. Duan, A. Elmali, Y. Hou, J. Zhao, G. G. Gurzadyan, A. Karatay, V. K. Voronkova, C. Li, *J. Phys. Chem. C* **2019**, *123*, 18270.
- [173] F. Zhong, J. Zhao, *Dyes Pigm.* **2017**, *136*, 909.
- [174] W. J. Shi, M. E. El-Khouly, K. Ohkubo, S. Fukuzumi, D. K. Ng, *Chem. - Eur. J.* **2013**, *19*, 11332.
- [175] Y. Zhao, R. Duan, J. Zhao, C. Li, *Chem. Commun.* **2018**, *54*, 12329.
- [176] Y. Dong, B. Dick, J. Zhao, *Org. Lett.* **2020**, *22*, 5535.
- [177] T. Jin, H. Li, K. Zhu, P.-F. Wang, P. Liu, L. Jiao, *Chem. Soc. Rev.* **2020**, *49*, 2342.
- [178] Y. Dong, A. A. Sukhanov, J. Zhao, A. Elmali, X. Li, B. Dick, A. Karatay, V. K. Voronkova, *J. Phys. Chem. C* **2019**, *123*, 22793.
- [179] J. Sun, X. Li, K. Du, F. Feng, *Chem. Commun.* **2018**, *54*, 9194.
- [180] Z. Mahmood, M. Taddei, N. Rehmat, L. Bussotti, S. Doria, Q. Guan, S. Ji, J. Zhao, M. Di Donato, Y. Huo, *J. Phys. Chem. C* **2020**, *124*, 5944.
- [181] N. Sekkat, H. V. D. Bergh, T. Nyokong, N. Lange, *Molecules* **2012**, *17*, 98.
- [182] W. Shao, C. Yang, F. Li, J. Wu, N. Wang, Q. Ding, J. Gao, D. Ling, *Nano-Micro Lett.* **2020**, *12*, 1.
- [183] Y.-F. Xiao, J.-X. Chen, S. Li, W.-W. Tao, S. Tian, K. Wang, X. Cui, Z. Huang, X.-H. Zhang, C.-S. Lee, *Chem. Sci.* **2020**, *11*, 888.
- [184] G. Han, T. Hu, Y. Yi, *Adv. Mater.* **2020**, *32*, 2000975.
- [185] S. Holliday, Y. Li, C. K. Luscombe, *Prog. Polym. Sci.* **2017**, *70*, 34.
- [186] S. Xu, Y. Yuan, X. Cai, C.-J. Zhang, F. Hu, J. Liang, G. Zhang, D. Zhang, B. Liu, *Chem. Sci.* **2015**, *6*, 5824.
- [187] V.-N. Nguyen, Y. Yan, J. Zhao, J. Yoon, *Acc. Chem. Res.* **2020**, *54*, 16243.
- [188] D. Musib, M. Pal, M. K. Raza, M. Roy, *Dalton Trans.* **2020**, *49*, 10786.
- [189] S. Liu, H. Zhang, Y. Li, J. Liu, L. Du, M. Chen, R. T. Kwok, J. W. Lam, D. L. Phillips, B. Z. Tang, *Angew. Chem., Int. Ed.* **2018**, *57*, 15189.
- [190] M. J. Leidl, V. A. Krylova, P. I. Djurovich, M. E. Thompson, H. Yersin, *J. Am. Chem. Soc.* **2014**, *136*, 16032.
- [191] D. M. Freeman, A. J. Musser, J. M. Frost, H. L. Stern, A. K. Forster, K. J. Fallon, A. G. Rapisdi, F. Cacialli, I. McCulloch, T. M. Clarke, *J. Am. Chem. Soc.* **2017**, *139*, 11073.
- [192] X. K. Liu, Z. Chen, C. J. Zheng, C. L. Liu, C. S. Lee, F. Li, X. M. Ou, X. H. Zhang, *Adv. Mater.* **2015**, *27*, 2378.
- [193] X. K. Liu, Z. Chen, J. Qing, W. J. Zhang, B. Wu, H. L. Tam, F. Zhu, X. H. Zhang, C. S. Lee, *Adv. Mater.* **2015**, *27*, 7079.
- [194] J. Zhang, W. Chen, R. Chen, X.-K. Liu, Y. Xiong, S. V. Kershaw, A. L. Rogach, C. Adachi, X. Zhang, C.-S. Lee, *Chem. Commun.* **2016**, *52*, 11744.
- [195] W. Chen, F. Song, *Chin. Chem. Lett.* **2019**, *30*, 1717.
- [196] K. Shizu, H. Tanaka, M. Uejima, T. Sato, K. Tanaka, H. Kaji, C. Adachi, *J. Phys. Chem. C* **2015**, *119*, 1291.
- [197] Q. Zhang, D. Tsang, H. Kuwabara, Y. Hatae, B. Li, T. Takahashi, S. Y. Lee, T. Yasuda, C. Adachi, *Adv. Mater.* **2015**, *27*, 2096.
- [198] T. H. Kwon, S. O. Jeon, M. Numata, H. Lee, Y. S. Chung, J. S. Kim, S.-G. Ihn, M. Sim, S. Kim, B. M. Kim, *Nanomater* **2019**, *9*, 1735.
- [199] S.-J. Woo, Y. Kim, Y.-H. Kim, S.-K. Kwon, J.-J. Kim, *J. Mater. Chem. C* **2019**, *7*, 4191.
- [200] H. Uoyama, K. Goushi, K. Shizu, H. Nomura, C. Adachi, *Nature* **2012**, *492*, 234.
- [201] J. Zhang, F. Fang, B. Liu, J.-H. Tan, W.-C. Chen, Z. Zhu, Y. Yuan, Y. Wan, X. Cui, S. Li, *ACS Appl. Mater. Interfaces* **2019**, *11*, 41051.
- [202] R. Ishimatsu, S. Matsunami, K. Shizu, C. Adachi, K. Nakano, T. Imato, *J. Phys. Chem. A* **2013**, *117*, 5607.
- [203] S. Haseyama, A. Niwa, T. Kobayashi, T. Nagase, K. Goushi, C. Adachi, H. Naito, *Nanoscale Res. Lett.* **2017**, *12*, 268.
- [204] N. G. Pschirer, C. Kohl, F. Nolde, J. Qu, K. Müllen, *Angew. Chem.* **2006**, *118*, 1429.
- [205] F. Charra, D. Fichou, J.-M. Nunzi, N. Pfeffer, *Chem. Phys. Lett.* **1992**, *192*, 566.
- [206] J.-M. Nunzi, *C. R. Phys.* **2002**, *3*, 523.
- [207] W.-R. Zhuang, Y. Wang, P.-F. Cui, L. Xing, J. Lee, D. Kim, H.-L. Jiang, Y.-K. Oh, *J. Controlled Release* **2019**, *294*, 311.
- [208] P. Acharya, J. Chattopadhyaya, *Pure Appl. Chem.* **2005**, *77*, 291.
- [209] L. Lin, L. Xiong, Y. Wen, S. Lei, X. Deng, Z. Liu, W. Chen, X. Miao, *J. Biomed. Nanotechnol.* **2015**, *11*, 531.
- [210] G. Zhu, G. Niu, X. Chen, *Bioconjugate Chem.* **2015**, *26*, 2186.
- [211] K. Wang, Y. Zhang, J. Wang, A. Yuan, M. Sun, J. Wu, Y. Hu, *Sci. Rep.* **2016**, *6*, 27421.
- [212] Q. Guan, L. Zhou, F. Lv, W. Li, Y. Li, Y. Dong, *Angew. Chem., Int. Ed.* **2020**, *59*, 18042.
- [213] S. Yan, D. Tang, Z. Hong, J. Wang, H. Yao, L. Lu, H. Yi, S. Fu, C. Zheng, G. He, H. Zou, X. Hou, Q. He, L. Xiong, Q. Li, X. Deng, *Biomater. Sci.* **2021**, *9*, 2020.
- [214] L. Dai, G. Shen, Y. Wang, P. Yang, H. Wang, Z. Liu, *J. Mater. Chem. B* **2021**, *9*, 1151.
- [215] C. Chung, K. Lu, W. Lee, W. Hsu, W. Lee, J. Dai, P. Shueng, C. Lin, F. Mi, *Biomater* **2020**, *257*, 120227.
- [216] T. Zhang, Z. Zhang, Y. Yue, X. Hu, F. Huang, L. Shi, Y. Liu, D. Guo, *Adv. Mater.* **2020**, *32*, 1908435.
- [217] J. Fang, H. Nakamura, H. Maeda, *Adv. Drug Delivery Rev.* **2011**, *63*, 136.
- [218] R. Allison, H. Mota, V. Bagnato, C. Sibata, *Photodiagn. Photodyn. Ther.* **2008**, *5*, 19.
- [219] S. Sindhvani, A. Syed, J. Ngai, B. Kingston, L. Maiorino, J. Rothschild, P. MacMillan, Y. Zhang, N. Rajesh, T. Hoang, J. Wu, S. Wilhelm, A. Zilman, S. Gadde, A. Sulaiman, B. Ouyang, Z. Lin, L. Wang, M. Egeblad, W. Chan, *Nat. Mater.* **2020**, *19*, 566.
- [220] X. Zhang, J. Tang, C. Li, Y. Lu, L. Cheng, J. Liu, *Bioact. Mater.* **2021**, *6*, 472.
- [221] Y. Yang, S. Wang, Y. Zhou, X. Wang, X. Liu, A. Xie, Y. Shen, M. Zhu, *Colloids Surf., B* **2020**, *196*, 111346.
- [222] W. Sharman, C. Allen, J. van Lier, *Methods Enzymol.* **2000**, *319*, 376.
- [223] D. Kessel, J. Reiners, *Photochem. Photobiol.* **2015**, *91*, 931.
- [224] T. Akhlynnina, D. Jans, A. Rosenkranz, N. Statsyuk, I. Balashova, G. Toth, I. Pavo, A. Rubin, A. Sobolev, *J. Biol. Chem.* **1997**, *272*, 20328.
- [225] H. Deng, Z. Zhou, W. Yang, L. Lin, S. Wang, G. Niu, J. Song, X. Chen, *Nano Lett.* **2020**, *20*, 1928.

- [226] J. Sun, K. Du, J. Diao, X. Cai, F. Feng, S. Wang, *Angew. Chem., Int. Ed.* **2020**, *59*, 12122.
- [227] S. Liang, C. Sun, P. Yang, P. Ma, S. Huang, Z. Cheng, X. Yu, J. Lin, *Biomater* **2020**, *240*, 119850.
- [228] Z. Liu, H. Zou, Z. Zhao, P. Zhang, G. Shan, R. Kwok, J. Lam, L. Zheng, B. Tang, *ACS Nano* **2019**, *13*, 11283.
- [229] M. Li, Y. Ning, J. Chen, X. Duan, N. Song, D. Ding, X. Su, Z. Yu, *Nano Lett.* **2019**, *19*, 7965.
- [230] C. Wang, X. Zhao, H. Jiang, J. Wang, W. Zhong, K. Xue, C. Zhu, *Nanoscale* **2021**, *13*, 1195.
- [231] L. Qiao, J. Liu, Y. Han, F. Wei, X. Liao, C. Zhang, L. Xie, L. Ji, H. Chao, *Chem. Commun.* **2021**, 57, 1790.
- [232] A. P. Castano, T. N. Demidova, M. R. Hamblin, *Photodiagn. Photodyn. Ther.* **2005**, *2*, 91.
- [233] F. Yuan, M. Leunig, D. A. Berk, R. K. Jain, *Microvasc. Res.* **1993**, *45*, 269.
- [234] I. Yoon, J. Z. Li, Y. K. Shim, *Clin. Endosc.* **2013**, *46*, 7.
- [235] M. Mora, M. L. Sagristá, *J. Porphyrins Phthalocyanines* **2009**, *13*, 537.
- [236] J. Li, X. Zhen, Y. Lyu, Y. Jiang, J. Huang, K. Pu, *ACS Nano* **2018**, *12*, 8520.
- [237] P. Escobar, A. M. Vera, L. F. Neira, A. O. Velásquez, H. Carreño, *Exp. Parasitol.* **2018**, *194*, 45.
- [238] D. K. Deda, K. Araki, *J. Braz. Chem. Soc.* **2015**, *26*, 2448.
- [239] M.-J. Shieh, C.-L. Peng, W.-L. Chiang, C.-H. Wang, C.-Y. Hsu, S.-J. Wang, P.-S. Lai, *Mol. Biopharm.* **2010**, *7*, 1244.
- [240] D. W. Deamer, *FASEB J.* **2010**, *24*, 1308.
- [241] C. K. Haluska, K. A. Riske, V. Marchi-Artzner, J.-M. Lehn, R. Lipowsky, R. Dimova, *Proc. Natl. Acad. Sci. USA* **2006**, *103*, 15841.
- [242] A. Gabizon, D. Papahadjopoulos, *Proc. Natl. Acad. Sci. USA* **1988**, *85*, 6949.
- [243] M. C. Woodle, *Adv. Drug Delivery Rev.* **1995**, *16*, 249.
- [244] M. L. Immordino, F. Dosio, L. Cattell, *Int. J. Nanomed.* **2006**, *1*, 297.
- [245] T. Allen, C. Hansen, F. Martin, C. Redemann, A. Yau-Young, *Biochim. Biophys. Acta, Biomembr.* **1991**, *1066*, 29.
- [246] D. C. Drummond, O. Meyer, K. Hong, D. B. Kirpotin, D. Papahadjopoulos, *Pharmacol. Rev.* **1999**, *51*, 691.
- [247] H. Maeda, T. Sawa, T. Konno, *J. Controlled Release* **2001**, *74*, 47.
- [248] C. Allen, N. Dos Santos, R. Gallagher, G. Chiu, Y. Shu, W. Li, S. Johnstone, A. Janoff, L. Mayer, M. Webb, *Biosci. Rep.* **2002**, *22*, 225.
- [249] P. Caliceti, F. M. Veronese, *Adv. Drug Delivery Rev.* **2003**, *55*, 1261.
- [250] X. Wang, J. Wang, J. Li, H. Huang, X. Sun, Y. Lv, *J. Drug Delivery Sci. Technol.* **2018**, *48*, 414.
- [251] S. P. Egusquiaguirre, M. Igartua, R. M. Hernández, J. L. Pedraz, *Clin. Transl. Oncol.* **2012**, *14*, 83.
- [252] F. Pourgholi, J.-N. Farhad, H. S. Kafil, M. Yousefi, *Biomed. Pharmacother.* **2016**, *77*, 98.
- [253] D. Depan, J. Shah, R. Misra, *Mater. Sci. Eng., C* **2011**, *31*, 1305.
- [254] W. Miao, G. Shim, S. Lee, S. Lee, Y. S. Choe, Y.-K. Oh, *Biomater* **2013**, *34*, 3402.
- [255] P. Huang, C. Xu, J. Lin, C. Wang, X. Wang, C. Zhang, X. Zhou, S. Guo, D. Cui, *Theranostics* **2011**, *1*, 240.
- [256] X. Sun, A. Zebibula, X. Dong, G. Zhang, D. Zhang, J. Qian, S. He, *ACS Appl. Mater. Interfaces* **2018**, *10*, 25037.
- [257] C. Dupont, A. S. Vignion, S. Mordon, N. Reyns, M. Vermandel, *Lasers Surg. Med.* **2018**, *50*, 523.
- [258] S. W. Cramer, C. C. Chen, *Front. Surg.* **2020**, *6*, 81.
- [259] D. Bartusik, D. Aebischer, A. Ghogare, G. Ghosh, I. Abramova, T. Hasan, A. Greer, *Photochem. Photobiol.* **2013**, *89*, 936.
- [260] J. H. Kang, Y. T. Ko, *Biomater. Sci.* **2019**, *7*, 2812.
- [261] A. Bansal, F. Yang, T. Xi, Y. Zhang, J. S. Ho, *Proc. Natl. Acad. Sci. USA* **2018**, *115*, 1469.
- [262] D. M. Kustov, P. V. Grachev, E. I. Kozlikina, V. B. Loschenov, *Int. Conf. Laser Opt. (ICLO) IEEE* **2020**, 1.
- [263] M. Agarwal, H. Larkin, S. Zaidi, H. Mukhtar, N. Oleinick, *Cancer Res.* **1993**, *53*, 5897.
- [264] N. Yamamoto, S. Homma, T. Sery, L. Donoso, J. Hooper, *Eur. J. Cancer* **1991**, *27*, 467.
- [265] P. Kousis, B. Henderson, P. Maier, S. Gollnick, *Cancer Res.* **2007**, *67*, 10501.
- [266] A. Kaczmarek, P. Vandenabeele, D. Krysko, *Immunity* **2013**, *38*, 209.
- [267] D. Krysko, A. Garg, A. Kaczmarek, O. Krysko, P. Agostinis, P. Vandenabeele, *Nat. Rev. Cancer* **2012**, *12*, 860.
- [268] L. Galluzzi, A. Buqué, O. Kepp, L. Zitvogel, G. Kroemer, *Nat. Rev. Immunol.* **2017**, *17*, 97.
- [269] L. Galluzzi, I. Vitale, S. Warren, S. Adjemian, P. Agostinis, A. Martinez, T. Chan, G. Coukos, S. Demaria, E. Deutsch, D. Draganov, R. Edelson, S. Formenti, J. Fucikova, L. Gabriele, U. Gaigl, S. Gameiro, A. Garg, E. Golden, J. Han, K. Harrington, A. Hemminki, J. Hodge, D. Hossain, T. Illidge, M. Karin, H. Kaufman, O. Kepp, G. Kroemer, J. Lasarte, et al., *Cancer* **2020**, *8*, e000337.
- [270] L. Galluzzi, O. Kepp, G. Kroemer, *EMBO J.* **2012**, *31*, 1055.
- [271] B. Doix, N. Trempolec, O. Riant, O. Feron, *Front. Oncol.* **2019**, *9*, 811.
- [272] P. Mroz, J. Hashmi, Y. Huang, N. Lange, M. Hamblin, *Expert Rev. Clin. Immunol.* **2011**, *7*, 75.
- [273] M. Yenari, J. Liu, Z. Zheng, Z. Vexler, J. Lee, R. Giffard, *Ann. N. Y. Acad. Sci.* **2005**, *1053*, 74.
- [274] D. Krysko, P. Agostinis, O. Krysko, A. Garg, C. Bachert, B. Lambrecht, P. Vandenabeele, *Trends Immunol.* **2011**, *32*, 157.
- [275] J. De Munck, A. Binks, I. McNeish, J. Aerts, *J. Leukocyte Biol.* **2017**, *102*, 631.
- [276] S. Todryk, A. Melcher, N. Hardwick, E. Linardakis, A. Bateman, M. Colombo, A. Stoppacciaro, R. Vile, *J. Immunol.* **1999**, *163*, 1398.
- [277] G. Deng, Z. Sun, S. Li, X. Peng, W. Li, L. Zhou, Y. Ma, P. Gong, L. Cai, *ACS Nano* **2018**, *12*, 12096.
- [278] Q. Guan, L. Zhou, Y. Li, W. Li, S. Wang, C. Song, Y. Dong, *ACS Nano* **2019**, *13*, 13304.
- [279] L. Zeng, Y. Pan, Y. Tian, X. Wang, W. Ren, S. Wang, G. Lu, A. Wu, *Biomater* **2015**, *57*, 93.
- [280] S. Kim, S. Kim, G. Nam, Y. Hong, G. Kim, Y. Choi, S. Lee, Y. Cho, M. Kwon, C. Jeong, S. Kim, I. Kim, *J. Immunother. Cancer* **2021**, *9*, e001481.
- [281] J. Liu, F. Hu, M. Wu, L. Tian, F. Gong, X. Zhong, M. Chen, Z. Liu, B. Liu, *Adv. Mater.* **2021**, *33*, 2007888.
- [282] B. Tian, C. Wang, S. Zhang, L. Feng, Z. Liu, *ACS Nano* **2011**, *5*, 7000.
- [283] Q. Xiao, X. Zheng, W. Bu, W. Ge, S. Zhang, F. Chen, H. Xing, Q. Ren, W. Fan, K. Zhao, Y. Hua, J. Shi, *J. Am. Chem. Soc.* **2013**, *135*, 13041.
- [284] Z. Wen, F. Liu, G. Liu, Q. Sun, Y. Zhang, M. Muhammad, Y. Xu, H. Li, S. Sun, *J. Colloid Interface Sci.* **2021**, *590*, 290.
- [285] H. Yang, B. Xu, S. Li, Q. Wu, M. Lu, A. Han, H. Liu, *Small* **2021**, *17*, e2007090.
- [286] P. Huang, L. Bao, C. Zhang, J. Lin, T. Luo, D. Yang, M. He, Z. Li, G. Gao, B. Gao, S. Fu, D. Cui, *Biomater* **2011**, *32*, 9796.
- [287] S. Wang, P. Huang, L. Nie, R. Xing, D. Liu, Z. Wang, J. Lin, S. Chen, G. Niu, G. Lu, X. Chen, *Adv. Mater.* **2013**, *25*, 3055.
- [288] Q. Liu, Z. Hu, M. Chen, C. Zou, H. Jin, S. Wang, S. L. Chou, Y. Liu, S. X. Dou, *Adv. Funct. Mater.* **2020**, *30*, 1909530.
- [289] X. Li, F. Fang, B. Sun, C. Yin, J. Tan, Y. Wan, J. Zhang, P. Sun, Q. Fan, P. Wang, S. Li, C. Lee, *Nanoscale Horiz.* **2021**, *6*, 177.
- [290] C. He, D. Liu, W. Lin, *ACS Nano* **2015**, *9*, 991.
- [291] Z. Wang, R. Ma, L. Yan, X. Chen, G. Zhu, *Chem. Commun.* **2015**, *51*, 11587.
- [292] C. Zhao, R. Cheng, Z. Yang, Z. Tian, *Molecules* **2018**, *23*, 826.
- [293] Q. Chen, Y. Ma, P. Bai, Q. Li, B. Canup, D. Long, B. Ke, F. Dai, B. Xiao, C. Li, *ACS Appl. Mater. Interfaces* **2021**, *13*, 4861.
- [294] P. Wang, C. Liang, J. Zhu, N. Yang, A. Jiao, W. Wang, X. Song, X. Dong, *ACS Appl. Mater. Interfaces* **2019**, *11*, 41140.

- [295] Z. Zhang, R. Wang, X. Huang, R. Luo, J. Xue, J. Gao, W. Liu, F. Liu, F. Feng, W. Qu, *ACS Appl. Mater. Interfaces* **2020**, *12*, 5680.
- [296] X. Cheng, L. He, J. Xu, Q. Fang, L. Yang, Y. Xue, X. Wang, R. Tang, *Acta Biomater* **2020**, *112*, 234.
- [297] X. Li, Y. Jeon, N. Kwon, J. Park, T. Guo, H. Kim, J. Huang, D. Lee, J. Yoon, *Biomater* **2021**, *266*, 120430.
- [298] H. Xu, Y. Han, G. Zhao, L. Zhang, Z. Zhao, Z. Wang, L. Zhao, L. Hua, K. Naveena, J. Lu, R. Yu, H. Liu, *ACS Appl. Mater. Interfaces* **2020**, *12*, 52319.
- [299] B. Ma, J. Sheng, P. Wang, Z. Jiang, E. Borrathybay, *Int. J. Nanomed.* **2019**, *14*, 4541.
- [300] L. Santos, J. Oliveira, E. Monteiro, J. Santos, C. Sarmiento, *Case Rep. Oncol.* **2018**, *11*, 769.
- [301] Q. Qiu, C. Li, X. Yan, H. Zhang, X. Luo, X. Gao, X. Liu, Y. Song, Y. Deng, *Biomater* **2021**, *269*, 120652.
- [302] Y. Zhou, X. Ren, Z. Hou, N. Wang, Y. Jiang, Y. Luan, *Nanoscale Horiz.* **2020**, *6*, 120.
- [303] J. Zhu, W. Wang, X. Wang, L. Zhong, X. Song, W. Wang, Y. Zhao, X. Dong, *Adv. Healthcare Mater.* **2021**, *10*, 2002038.
- [304] X. Wu, H. Yang, X. Chen, J. Gao, Y. Duan, D. Wei, J. Zhang, K. Ge, X. Liang, Y. Huang, S. Feng, R. Zhang, X. Chen, J. Chang, *Biomater* **2021**, *269*, 120654.
- [305] J. Huang, Y. Huang, Z. Xue, S. Zeng, *Biomater* **2020**, *262*, 120346.
- [306] T. Jia, Z. Wang, Q. Sun, S. Dong, J. Xu, F. Zhang, L. Feng, F. He, D. Yang, P. Yang, J. Lin, *Small* **2020**, *16*, e2001343.
- [307] Y. Hao, W. Zhang, Y. Gao, Y. Wei, Y. Shu, J. Wang, *J. Mater. Chem. B* **2021**, *9*, 250.
- [308] S. Liu, W. Li, S. Dong, F. Zhang, Y. Dong, B. Tian, F. He, S. Gai, P. Yang, *Nanoscale* **2020**, *12*, 24146.
- [309] Q. Ding, Y. Liu, C. Shi, J. Xiao, W. Dai, D. Liu, H. Chen, B. Li, J. Liu, *Mini-Rev. Med. Chem.* **2021**, *21*, 1718.
- [310] Q. Zheng, X. Liu, Y. Zheng, K. Yeung, Z. Cui, Y. Liang, Z. Li, S. Zhu, X. Wang, S. Wu, *Chem. Soc. Rev.* **2021**.
- [311] C. Sui, R. Tan, Y. Chen, G. Yin, Z. Wang, W. Xu, X. Li, *Bioconjugate Chem.* **2021**, *32*, 318.
- [312] J. Ding, G. Lu, W. Nie, L. Huang, Y. Zhang, W. Fan, G. Wu, H. Liu, H. Xie, *Adv. Mater.* **2021**, *33*, 2005562.
- [313] K. Bennewith, S. Dedhar, *BMC Cancer* **2011**, *11*, 504.
- [314] R. Kumari, D. Sunil, R. Ningthoujam, N. Kumar, *Chem.-Biol. Interact.* **2019**, *307*, 91.
- [315] W. Tang, Z. Zhen, M. Wang, H. Wang, Y. Chuang, W. Zhang, G. Wang, T. Todd, T. Cowger, H. Chen, L. Liu, Z. Li, J. Xie, *Adv. Funct. Mater.* **2016**, *26*, 1757.
- [316] T. Li, X. Jing, Y. Huang, *Macromol. Biosci.* **2011**, *11*, 865.
- [317] X. Guo, J. Qu, C. Zhu, W. Li, L. Luo, J. Yang, X. Yin, Q. Li, Y. Du, D. Chen, Y. Qiu, Y. Lou, J. You, *Drug Delivery* **2018**, *25*, 585.
- [318] Z. Luo, H. Tian, L. Liu, Z. Chen, R. Liang, Z. Chen, Z. Wu, A. Ma, M. Zheng, L. Cai, *Theranostics* **2018**, *8*, 3584.
- [319] L. O'Connor, C. Cazares-Körner, J. Saha, C. Evans, M. Stratford, E. Hammond, S. Conway, *Nat. Protoc.* **2016**, *11*, 781.
- [320] F. Hunter, B. Wouters, W. Wilson, *Br. J. Cancer* **2016**, *114*, 1071.
- [321] L. Feng, L. Cheng, Z. Dong, D. Tao, T. Barnhart, W. Cai, M. Chen, Z. Liu, *ACS Nano* **2017**, *11*, 927.
- [322] S. Zhou, X. Hu, R. Xia, S. Liu, Q. Pei, G. Chen, Z. Xie, X. Jing, *Angew. Chem., Int. Ed.* **2020**, *59*, 23198.
- [323] M. Shirmanova, D. Yuzhakova, L. Snopova, G. Perelman, E. Serebrovskaya, K. Lukyanov, I. Turchin, P. Subochev, S. Lukyanov, V. Kamensky, E. Zagaynova, *PLoS One* **2015**, *10*, e0144617.
- [324] M. Yuan, C. Liu, J. Li, W. Ma, X. Yu, P. Zhang, Y. Ji, *BMC Cancer* **2019**, *19*, 934.
- [325] M. Micheletto, É. Guidelli, A. Costa-Filho, *ACS Appl. Mater. Interfaces* **2021**, *13*, 2289.
- [326] A. Holmes, L. Moore, A. Sundsfjord, M. Steinbakk, S. Regmi, A. Karkey, P. Guerin, L. Piddock, *Lancet* **2016**, *387*, 176.
- [327] H. Gelband, R. Laxminarayan, *Trends Microbiol.* **2015**, *23*, 524.
- [328] M. Baym, T. Lieberman, E. Kelsic, R. Chait, R. Gross, I. Yelin, R. Kishony, *Science* **2016**, *353*, 1147.
- [329] E. Garcia, N. Ly, J. Diep, G. Rao, *Clin. Pharmacol. Ther.* **2021**.
- [330] C. Nathan, *Nat. Rev. Microbiol.* **2020**, *18*, 259.
- [331] Y. Zhang, P. Huang, D. Wang, J. Chen, W. Liu, P. Hu, M. Huang, X. Chen, Z. Chen, *Nanoscale* **2018**, *10*, 15485.
- [332] C. Li, F. Lin, W. Sun, F. Wu, H. Yang, R. Lv, Y. Zhu, H. Jia, C. Wang, G. Gao, Z. Chen, *ACS Appl. Mater. Interfaces* **2018**, *10*, 16715.
- [333] L. Ning, P. Liu, B. Wang, C. Li, E. Kang, Z. Lu, X. Hu, L. Xu, *J. Colloid Interface Sci.* **2019**, *549*, 72.
- [334] J. Huang, M. Guo, S. Jin, M. Wu, C. Yang, G. Zhang, P. Wang, J. Ji, Q. Zeng, X. Wang, H. Wang, *Photodiagn. Photodyn. Ther.* **2019**, *28*, 330.
- [335] M. Jia, B. Mai, S. Liu, Z. Li, Q. Liu, P. Wang, *Photodiagn. Photodyn. Ther.* **2019**, *28*, 80.
- [336] B. Sharma, G. Kaur, G. Chaudhary, S. Gawali, P. Hassan, *Biomater. Sci.* **2020**, *8*, 2905.
- [337] K. Shitomi, H. Miyaji, S. Miyata, T. Sugaya, N. Ushijima, T. Akasaka, H. Kawasaki, *Photodiagn. Photodyn. Ther.* **2020**, *30*, 101647.
- [338] Y. Matsushima, A. Yashima, M. Fukaya, S. Shirakawa, T. Ohshima, T. Kawai, T. Nagano, K. Gomi, *Antibiotics* **2021**, *10*, 101.
- [339] T. Yang, Y. Tan, W. Zhang, W. Yang, J. Luo, L. Chen, H. Liu, G. Yang, X. Lei, *Front. Cell Dev. Biol.* **2020**, *8*, 585132.
- [340] L. Hong, X. Liu, L. Tan, Z. Cui, X. Yang, Y. Liang, Z. Li, S. Zhu, Y. Zheng, K. Yeung, D. Jing, D. Zheng, X. Wang, S. Wu, *Adv. Healthcare Mater.* **2019**, *8*, e1900835.
- [341] Z. Zhao, R. Yan, J. Wang, H. Wu, Y. Wang, A. Chen, S. Shao, Y. Li, *J. Mater. Chem. B* **2017**, *5*, 3572.
- [342] C. Lu, F. Sun, Y. Liu, Y. Xiao, Y. Qiu, H. Mu, J. Duan, *Carbohydr. Polym.* **2019**, *218*, 289.
- [343] L. Mei, X. Gao, Y. Shi, C. Cheng, Z. Shi, M. Jiao, F. Cao, Z. Xu, X. Li, J. Zhang, *ACS Appl. Mater. Interfaces* **2020**, *12*, 40153.



**Mr. Zheng Yang Jin** is currently a masters student at Wenzhou Medical University in China. His research focuses on the combination of photodynamic therapy and nanotechnology with clinical practice to improve the prognosis of a variety of diseases, mainly cancer. He has a strong interest in material-based medical treatment mode, hoping to better combine the cutting-edge material technology with clinical practice.



**Mrs. Hira Fatima** is currently a Ph.D. candidate at Curtin University, Australia. Her research focuses on developing functional materials for biomedical and water treatment applications, for example, magnetic resonance imaging, magnetic hyperthermia, photodynamic therapy, and photocatalysis. Her primary interests are material designs based on the rational modification of structural and morphological properties of the functional materials.